Computation of K-shell X-ray Fluorescence Cross Section for photons ranging from 5.46 keV to 123.6 keV using three-dimensional semi-empirical formulae

K. Amari[1,2], A. Kahoul[1,2*], J.M. Sampaio[3,4], S. Daoudi[1,2], J.P. Marques[3,4], F. Parente[5], A. Hamidani[1,2], S. Croft[6], A. Favalli[7,8], Y. Kasri[9,10], A. Zidi[1,2], B. Berkani[1,2]

[1]*Department of Matter Sciences, Faculty of Sciences and Technology, Mohamed El Bachir El Ibrahimi University, Bordj-Bou-Arreridj 34030, Algeria.*
[2]*Laboratory of Materials Physics, Radiation and Nanostructures (LPMRN), Faculty of Sciences and Technology, Mohamed El Bachir El Ibrahimi University, Bordj-Bou-Arreridj 34030, Algeria.*
[3]*LIP – Laboratório de Instrumentação e Física Experimental de Partículas, Av. Prof. Gama Pinto 2, 1649-003 Lisboa, Portugal.*
[4]*Faculdade de Ciências da Universidade de Lisboa, Campo Grande, C8, 1749-016 Lisboa, Portugal.*
[5]*Laboratory of Instrumentation, Biomedical Engineering and Radiation Physics (LIBPhys-UNL), Department of Physics, NOVA School of Science and Technology, NOVA University Lisbon, 2829-516 Caparica, Portugal.*
[6]*School of Engineering, Faculty of Science of Technology, Nuclear Science, Engineering Research Group, Lancaster University, Bailrigg, Lancaster, LA1 4YW, United Kingdom.*
[7]*European Commission, Joint Research Centre, Ispra, I-21027, Italy.*
[8]*Los Alamos National Laboratory, P.O. Box 1663, Los Alamos, NM 87545, USA.*
[9]*Department of Physics, Faculty of Sciences, University of Mohamed Boudiaf, 28000 M'sila, Algeria.*
[10] *Theoretical Physics Laboratory, Faculty of Exact Sciences, Bejaia University, 06000 Bejaia, Algeria*
[*]Corresponding author. Tel. /Fax (+213) 035862230.
E-mail address: a.kahoul@univ-bba.dz; ahalim.kahoul@gmail.com

Abstract:

In this work, we propose a novel three-dimensional semi-empirical formula for the estimation of K-shell X-ray fluorescence cross sections for a wide range of elements $16 \leq Z \leq 92$ based on the database of the experimental values published between 1985 and 2023 for photons spanning from 5.46 to 123.6 keV (over 3300 data). This approach employs an analytical dependent on the atomic number Z and the energy E. Subsequently, the ratio $S_W = (\sigma_{Ki-Exp})/(\sigma_{Ki-W})$ are fitted using a three-dimension polynomial function, in terms of the atomic number Z and energy E. The cross-sections were described as the product of two functions, the first is a polynomial that represents the weighted mean of cross-sections values across different conditions and the second function provides additional fitting to the cross-section based on atomic numbers Z and energy E. The cross-sections expressed as function of these two variables show reasonable agreement with the experimental values.

Keywords: K-shell, XRF cross sections, semi-empirical calculation and fitting process.

1. Introduction

X-ray fluorescence is a fundamental physical phenomenon with a wide range of applications in atomic physics, analytical chemistry, materials science and many other areas of scientific research and industry (Scofield (1973), Hubbell and Seltzer (1995), Berger *et al*. (2010)). K-shell fluorescence cross sections are the most important and frequently the most crucial for many applications, including radiation dosimetry and non-destructive assays. The intensity and spectral characteristics of this fluorescence depend intimately on the properties of the atom in question.

One of the major challenges in the study of X-ray fluorescence lies in the precise calculation of the fluorescence cross section, which quantifies the probability that a fluorescent photon will be emitted by a given atom under a specific experimental condition. These conditions include important parameters such as the incident beam energy, the incidence and detection angle which influence the intensity and direction of the emitted X-rays, as well as the state of the target (solid, liquid, or gas) and its purity and thickness. Also, the detector type and its resolution, such as Si (Li) or HPGe detectors, play a crucial role in accuracy of fluorescent photon detection. Theoretically, the fundamental factors taken into account while determining the fluorescence cross section are photoionization cross sections, radiative rates, fluorescence yields, and Coster Kronig yields (Krause *et al*. (1978)).

In this context, semi-empirical calculations of the K-shell X-ray fluorescence cross section (K-XRFCSs) are a fundamental tool for predicting and interpreting X-ray intensities and associated spectra. The key advantage of this approach resides in its ability to produce accurate estimates of the K-shell X-ray fluorescence cross section for a wide range of elements and photon energies. Over time, a variety of theoretical models and empirical or semi-empirical approaches have been employed to determine these K-shell X-ray fluorescence cross sections. For instance, Krause *et al*. (1978) focused on the compilation of a theoretical table which gives

a comprehensive set of K-XRFCSs, along with useful formulae and essential parameters for calculating these cross sections whereas Puri *et al*. (1995) have provided an extensive table of empirical K shell (13≤ Z ≤ 92) and L series (35≤ Z ≤92) XRF cross sections at incident photon energy range 1-200 keV.

Several studies were done at the 59.5 keV excitation energy from ^{241}Am source. Doğan *et al*. (2013) have conducted the experimental and semi-empirical calculations of K_α and K_β XRFCSs of $_{24}$Cr and $_{30}$Zn. Experimental, theoretical and semi-empirical values of K_α and K_β XRFCSs for the same elements have been estimated by Dogan *et al*. (2014). Uğurlu and Demir (2020) has determined K X-ray fluorescence parameters, including fluorescence cross-section, vacancy transfer probabilities and fluorescence yield, of some fourth period elements in a magnetic field. Turhan and Akman (2023) have extensively investigated on the measurement of K-shell XRF parameters, such as cross sections (σ_{K_α} , σ_{K_β} and σ_K), and K_β/K_α intensity ratios, for some elements with $22 \leq Z \leq 48$.

In this paper, over 3300 measured K-shell XRFCS data (1049 for K_α, 999 for K_β and 1040 for K_{tot}) reported from different sources over the period 1985-2023 by photon impact were used to estimate the semi-empirical calculation of the K-shell X-ray fluorescence cross-section for the elements with $16 \leq Z \leq 92$ for photons ranging from 5.46 keV to 123.6 keV. The atomic number Z-range and energy E-range were selected because of the availability of experimental data. To derive a new semi-empirical scheme, the weighted average values were fitted using an interpolation method that involves the analytical function dependent on the atomic number Z and the energy E. Subsequently, the ratio $S_W = (\sigma_{Ki-Exp})/(\sigma_{Ki-W})$ was fitted using a three-dimension analytical polynomial function, using the variables Z and energy E. The results obtained were tabulated and compared with further empirical and experimental data.

3. Method of the semi-empirical calculation

To determine reliable semi-empirical and empirical K-shell X-ray production cross sections, the ideal situation is to perform the fitting of the experimental data for all elements across the given energy range. In this study, the semi-empirical formula is calculated using the same released experimental data as were used to calculate the empirical K-shell X-ray fluorescence cross-section. In our recent paper (Amari *et al*. (2024b)) we have estimated the empirical values by introducing a three-dimensional ($\sigma_{K_i}(Z,E)$) analytical function. Here we generalize this formula to interpolate the weighted average values for the K_α, K_β and K_{tot} X-ray fluorescence cross section. Afterward, we plotted the quantity (σ_{Ki-W}) as a function of atomic number Z and energy E. We next used an analytical function to fit these data, as follows:

$$(\sigma_{Ki-W}) = g(Z,E) \times f(Z) \quad (1)$$

where,

$g(Z,E) = c.Z^5.E^{-d}$, and f(Z) is a simple third-degree polynomial given as:

$$f(Z) = \sum_n a_n Z^n = a_0 + a_1 Z + a_2 Z^2 + a_3 Z^3 \quad (2)$$

Further, we plotted the ratio S against the energy E and the atomic number Z, and then fitted the data using the following formula:

$$S_W = \frac{(\sigma_{Ki-Exp})}{(\sigma_{Ki-W})} = P(Z) \times Q(E) \quad (3)$$

where

P(Z) is a second-order polynomial and Q(E) is a third-degree polynomial given by the following expressions:

$$P(Z) = \sum_i b_i Z^i = b_0 + b_1 Z + b_2 Z^2 \quad (4)$$

$$Q(E) = \sum_j l_j E^j = l_0 + l_1 E + l_2 E^2 + l_3 E^3 \quad (5)$$

Eventually, from equations (1) and (3) we deduced that the semi-empirical K-XRFCSs is estimated as follow:

$$\left(\sigma_{K_i}\right)_{Sem-emp} = (\sigma_{Ki-W}) \times S_W \quad (6)$$

The fitting coefficients for equations (1) and (3) are listed in Table. 1

For a more detailed explanation of the methodology used in this study, see the paper of (Amari *et al*. (2025)), which discussed the semi-empirical and empirical compilation of the partial K_{α_1}, K_{α_2}, $K_{\beta'_1}$ and $K_{\beta'_2}$ cross-sections using three-dimensional formulae.

The deviation of the experimental data $(\sigma_{Ki-Exp})$from their corresponding fitted values $(\sigma_{K_i})_{S-emp}$ is measured using the root-square errors ε_{rms}(%) as follows:

$$\varepsilon_{rms} = \left[\sum_{i=1}^{N} \frac{1}{N}\left(\frac{(\sigma_{Ki-Exp})-(\sigma_{K_i})_{S-emp}}{(\sigma_{K_i})_{S-emp}}\right)^2\right]^{1/2} \quad (7)$$

where N is the number of data points.

4. Results and discussion

In our recent papers (Amari *et al*. (2024b) and Amari *et al*. (2025)), we derived new empirical X-ray fluorescence cross-section values as well as the empirical and semi-empirical partial K_{α_1}, K_{α_2}, $K_{\beta'_1}$ and $K_{\beta'_2}$ cross-sections using a three-dimensional analytical function that as a function of Z and E. The database used in this work to determine the semi-empirical K_α, K_β and K_{tot} XRF cross-sections for targets with atomic numbers spanning from $_{16}$S to $_{92}$U and photon energies from 5.46 to 123.6 keV relies on the experimental data compilations recently published by our group (Amari *et al*. (2024a)). In order to produce reliable and consistent empirical values for σ_{K_α}, σ_{K_β} and $\sigma_{K_{tot}}$ XRFCSs and to achieve a satisfactory fitting, we divided the energy range into two parts: the first extends from 5.46 to 60 keV and the second spans from 60 to 123.6 keV. The fitting coefficients of Eq.s (1) and (3) and their corresponding root-mean-square errors within each energy range are listed in Table. 1. It is important to

emphasize that the fitting equation (6) and its associated parameters are valid only within the region of the experimental data used. Besides, this fitting formula and their coefficients are only valid across the photon energy range 5.46-123.6 keV. Extending this fitting beyond the specified ranges might lead to inaccurate and an unpredictable semi-empirical cross-section value. The fitting results are illustrated in Fig.s 1-12. We also note that the scatter observed in Fig.s 1-12 can be attributed to the fact that the data were taken from various references and sources, each measured different experimental condition. Tables 2-4 present the comparison between the current semi-empirical cross-section, the empirical values of Amari *et al.* (2024b) and other experimental values for selected elements namely, $_{28}$Ni, $_{38}$Sr, $_{42}$Mo, and $_{51}$Sb.

It is essential that the number of free parameters in a model be fewer that the number of data points, and the dynamic range must be sufficient to accurately capture the shape of the data. For example, it would be pointless to try and fit a third order polynomial in Z to 100 data points if all the points were for $Z = 47$. It is the number of Z 'clusters' that must exceed the number of free parameters. This is why we have opted for lower-order polynomials to prevent artificial patterns resulting from overfitting.

For each Z, a statistical study can determine a single 'optimal value' for use in the fit. In contrast the fitting process itself performs this 'weighting' automatically. It places greater emphasis on areas where the data is most densely populated and dependable. While it's important to recognize that the fits are semi-empirical and not based in a comprehensive physical model, they remain strong, and their reliability can be fairly gauged by examining the observed deviations.

For much of the fitted data, multiple values may exist at a specific E for a given Z, and as previously mentioned, one could opt to reduce this data to a single point before fitting. Nevertheless, the mathematical principles underlying the fitting process inherently perform this smoothing or averaging automatically.

Moreover, we aim to compare our semi-empirical K_α, K_β and K_{tot} XRFCSs findings with those from other experimental studies reported from the literature for selected elements, namely $_{28}$Ni, $_{38}$Sr, $_{42}$Mo and $_{51}$Sb. The comparison results for σ_{K_α}, σ_{K_β} and $\sigma_{K_{tot}}$ X-ray fluorescence cross-sections are presented in Fig.s 13-15, respectively. We notice that the selection of these elements is based on the availability of comprehensive experimental datasets.

It is worth noting that the formula used to compare our results with other experimental findings is given as follows:

$$D(\%) = \left| \frac{(\sigma_{Ki-Exp}) - (\sigma_{K_i})_{S-emp}}{(\sigma_{K_i})_{S-emp}} \right| \times 100$$

Through the analysis of the Fig.s 13-15, we conclude that:

For K_α line, it can be clearly seen from Fig. 13 that our semi-empirical results exhibit a strong consistency with the empirical values obtained by Amari *et al*. (2024b) across the specified energy range. Within the error range of these calculations, the deviation varies from 0.25% to 8.24% for $_{28}$Ni, from 0.26% to 3.58% for $_{38}$Sr, from 0.04% to 3.89% for $_{42}$Mo, and from 0.23% to 3.47% for $_{51}$Sb. Besides, the derived semi-empirical values at an excitation energy of 59.5 keV agree quit well with the experimental values of Demir and Şahin (2013) for elements $_{38}$Sr, $_{42}$Mo and $_{51}$Sb (the deviation is about 11% for $_{38}$Sr, between 5.16% and 9.67% for $_{42}$Mo, and between 2.20% and 6.30% for $_{51}$Sb), except for $_{28}$Ni where the deviation is up to 26%. In addition, our calculation shows a high degree of correlation with the experimental data of Baydaş *et al*. (2003) within the error range of 2.07% to 14.89% for $_{28}$Ni whereas a small deviation has been observed between our semi-empirical values and the experimental values of Rao *et al*. (1993) for photon energy ranging from 23.62 to 43.95 keV where the deviations extend from 19.72% to 24.12%. Further, for Strontium $_{38}$Sr our findings are in close agreement with the experimental values reported by Singh *et al*. (1990) with the deviation of 0.82% to 11.26%, except for the photon energy of 46.9 keV where the deviation is about 21.81%. Also,

a comparison between the estimated semi-empirical cross-sections and Seven's (Seven (2012)) measured values indicates a good agreement within the error range of 0.47% to 12.53% for $_{38}$Sr, 0.04% to 9.48% for $_{42}$Mo, and from 1.72% to 16.40% for $_{51}$Sb. Moreover, the obtained semi-empirical values from the whole energy range demonstrate good concordance with the measured values of Seven and Erdoğan (2015). Although, a deviation of 3.77% to 9.19% and 1.05% to 5.67% are observed for $_{42}$Mo and $_{51}$Sb, respectively.

For K_β line, from Fig. 14 we observe that the semi-empirical values deduced from formula (6) coincide very well with the empirical values published by Amari *et al*. (2024b) over the whole energy range used for elements $_{28}$Ni, $_{38}$Sr, $_{42}$Mo, and $_{51}$Sb (the deviations span from 1.04% to 13.31% for $_{28}$Ni, 0.40% to 11.55% for $_{38}$Sr, from 0.18% to 7.07% for $_{42}$Mo, and 0.07% to 6.58% for $_{51}$Sb). However, for Nickel, a slight variation is observed, with deviations spanning from 17.58% to 24.30% over the energy range of 36.82 to 59.5 keV.–Furthermore, for $_{28}$Ni the agreement between the present semi-empirical values and the experimental values of Baydaş *et al*. (2003) is quite satisfactory within the error range of 1.04% to 15.98%, except for the photon energy of 8.74 keV where the deviation is about 24.34%. However, a notable discrepancy is observed between our results and the experimental values of Rao *et al*. (1993) for photon energy of 43.95 keV where the deviation is up to 31.68%. Our calculations closely align with the measured data of Demir and Şahin (2013) for elements $_{38}$Sr, $_{42}$Mo, and $_{51}$Sb. The error range is approximately 7% for $_{51}$Sb, vary from 2.40% to 7.33% for $_{38}$Sr, and range from 0 to 10% for $_{42}$Mo. In contrast, more significant differences are seen for $_{28}$Ni, where the deviation reaches up to 24%. Besides, the semi-empirical values derived in this work correlate strongly with Seven's experimental values for a whole range of photon energy for elements $_{38}$Sr, $_{42}$Mo, and $_{51}$Sb. In this case the deviation ranges from 2.34% to 9.97% for $_{38}$Sr, vary from 1.99% to 11.10% from $_{42}$Mo, and span from 7.95% to 20.94% for $_{51}$Sb. In addition, the agreement between our findings and the measured values of Seven and Erdoğan (2015) is

reasonably good within the error range of 6.95% to 15.19% for $_{42}$Mo and 0.21% to 14.21% for $_{51}$Sb. Also, for $_{38}$Sr a reasonably good concordance is observed between our semi-empirical cross-sections and the experimental values of Singh *et al*. (1990) with deviation of 4.42% to 16.95% while a minor difference is observed at an excitation energy of 22.6 keV, where the deviation is about 24.42%.

For K_{tot} line, Fig. 15 clearly shows that there is a strong correspondence between the current semi-empirical cross-sections and the empirical values reported recently by our group (Amari *et al*. (2024b)) across the entire energy range. Considering the margin of error of these calculations, the deviations vary from 0.14% to 8.09% for $_{28}$Ni, from 0.01% to 3.51% for $_{38}$Sr, from 0.08% to 2.65% for $_{42}$Mo, and from 0.39% to 2.06% for $_{51}$Sb. Our results show a close agreement with the experimental values reported by Seven, 2012 for $_{38}$Sr, $_{42}$Mo, and $_{51}$Sb (the deviation spans from 4.89% to 13.47% for $_{38}$Sr, 0.98% to 7.57% for $_{42}$Mo, and range from 3.40% to 11.70% for $_{51}$Sb). Additionally, a strong correlation was obtained between our data and the values provided by Seven and Erdoğan (2015), with error ranges of 3.97% to 11.40% for $_{42}$Mo and 1% to 5.52% for $_{51}$Sb. Moreover, our semi-empirical values calculated at an excitation energy of 59.5 keV show a good agreement with the experimental data obtained by Demir and Şahin (2013) for $_{38}$Sr, $_{42}$Mo, and $_{51}$Sb where the deviations are up to 13% for $_{38}$Sr, between 7.19% and 12.29% for $_{42}$Mo, and between 0.43% to 9.63% for $_{51}$Sb. Nevertheless, a notable discrepancy is found for Nickel where the deviation is as high as 30%. Further, for $_{38}$Sr our semi-empirical values agree quite well with the experimental values of Singh *et al*. (1990) within the error range of 0.38% to 10.43% whereas a distinctive difference with the deviation of 22.39% is observed at a photon energy of 45.47 keV. For $_{28}$Ni, a significant consistency is found between the semi-empirical values determined in this work and the experimental values reported by Baydaş *et al*. (2003) across the energy range, with deviations of 0.43% to 12.16%.

However, the cross-sections findings derived from Eq. (6) have a worse agreement with the experimental values of Rao *et al*. (1993), where the deviation ranges from 16.24% to 21.37%.

5. Conclusion

Semi-empirical values of X-ray fluorescence cross-sections for K_α, K_β and K_{tot} lines are deduced using three-dimensional interpolation from experimental data extracted from various sources published between 1985 and 2023 (encompassing around 3300 experimental data), covering a wide range of elements $16 \leq Z \leq 92$ and by photon impact spanning from 5.46 to 123.6 keV.

The new semi-empirical values for the selected elements, namely $_{28}$Ni, $_{38}$Sr, $_{42}$Mo, and $_{51}$Sb were compared with the empirical findings published recently by our group and with other experimental works. This estimated show relatively in good agreement with those obtained by other groups across the entire range of photon energy. The proposed fit covers a wide dynamic range and is straightforward to apply.

Our systematic survey of the entire experimental data base highlights the need of new measurements in certain regions (Lanthanides ($58 \leq Z \leq 71$) at low energies ($< 40keV$)). Additionally, state-of-the-art calculations across the entire Z and E are essential.

Acknowledgments

We gratefully acknowledge the support of the DGRSDT, Ministry of Higher Education and Scientific Research, Algeria. This work was done with the support of Mohamed El Bachir El Ibrahimi University, under project (PRFU) N°: B00L02UN340120230003. This work was also supported by the Fundação para a Ciência e Tecnologia (FCT), Portugal through contracts UIDP/50007/2020 (LIP) and UID/FIS/04559/2020 (LIBPhys). S.C. warmly acknowledges the financial support of Lancaster University, and A.F. gratefully acknowledges the support of the Joint Research Centre of the European Commission.

Figures captions

Fig. 1. The distribution of the weighted average ($\sigma_{K\alpha-W}$) XRFCS values against atomic number *Z* and photon energy range of 5.46-59.5 keV. The fits are also represented by a surface.

Fig. 2. The distribution of the weighted average ($\sigma_{K\alpha-W}$) XRFCS values against atomic number *Z* and photon energy range of 59.5-123.6 keV. The fits are also represented by a surface.

Fig. 3. The distribution of the weighted average ($\sigma_{K\beta-W}$) XRFCS values against atomic number *Z* and photon energy range of 5.46-59.5 keV. The fits are also represented by a surface.

Fig. 4. The distribution of the weighted average ($\sigma_{K\beta-W}$) XRFCS values against atomic number *Z* and photon energy range of 59.5-123.6 keV. The fits are also represented by a surface.

Fig. 5. The distribution of the weighted average (σ_{Ktot-W}) XRFCS values against atomic number *Z* and photon energy range of 5.46-59.5 keV. The fits are also represented by a surface.

Fig. 6. The distribution of the weighted average (σ_{Ktot-W}) XRFCS values against atomic number *Z* and photon energy range of 59.5-123.6 keV. The fits are also represented by a surface.

Fig. 7. Distribution of the ratio $S_W = (\sigma_{K\alpha-Exp})/(\sigma_{K\alpha-W})$ according to the atomic number *Z* and photon energy range of 5.46-59.5 keV. The fits are also represented by a surface.

Fig. 8. Distribution of the ratio $S_W = (\sigma_{K\alpha-Exp})/(\sigma_{K\alpha-W})$ according to the atomic number *Z* and photon energy range of 59.5-123.6 keV. The fits are also represented by a surface.

Fig. 9. Distribution of the ratio $S_W = (\sigma_{K\beta-Exp})/(\sigma_{K\beta-W})$ according to the atomic number *Z* and photon energy range of 5.46-59.5 keV. The fits are also represented by a surface.

Fig. 10. Distribution of the ratio $S_W = (\sigma_{K\beta-Exp})/(\sigma_{K\beta-W})$ according to the atomic number *Z* and photon energy range of 59.5-123.6 keV. The fits are also represented by a surface.

Fig. 11. Distribution of the ratio $S_W = (\sigma_{Ktot-Exp})/(\sigma_{Ktot-W})$ according to the atomic number Z and photon energy range of 5.46-59.5 keV. The fits are also represented by a surface.

Fig. 12. Distribution of the ratio $S_W = (\sigma_{Ktot-Exp})/(\sigma_{Ktot-W})$ according to the atomic number Z and photon energy range of 59.5-123.6 keV. The fits are also represented by a surface.

Fig. 13. A comparison between semi-empirical K_α XRFCSs results deduced using Eq. (6), the empirical values of Amari *et al*. (2024b) and other experimental findings as a function of the photon energy for $_{28}$Ni, $_{38}$Sr, $_{42}$Mo and $_{51}$Sb.

Fig. 14. A comparison between semi-empirical K_β XRFCSs results deduced using Eq. (6), the empirical values of Amari *et al*. (2024b) and other experimental findings as a function of the photon energy for $_{28}$Ni, $_{38}$Sr, $_{42}$Mo and $_{51}$Sb.

Fig. 15. A comparison between semi-empirical K_{tot} XRFCSs results deduced using Eq. (6), the empirical values of Amari *et al*. (2024b) and other experimental findings as a function of the photon energy for $_{28}$Ni, $_{38}$Sr, $_{42}$Mo and $_{51}$Sb.

References

Amari, K., Kahoul, A., Sampaio, J.M., Kasri, Y., Marques, J.P., Parente, F., Hamidani, A., Croft, S., Favalli, A., Daoudi, S., Zidi, A., Berkani, B., 2025. Compilation of empirical and semi-empirical K_{α_1}, K_{α_2} , $K_{\beta'_1}$ and $K_{\beta'_2}$ X-ray fluorescence cross-sections by the application of fitting approaches. J. Quant. Spectrosc. Radiat. Transf. 337, 109393.

Amari, K., Kahoul, A., Sampaio, J.M., Daoudi, S., Marques, J.P., Parente, F., Hamidani, A., Croft, S., Favalli, A., Kasri, Y., Zidi, A., Berkani, B., 2024a. Experimental K-shell fluorescence cross sections for elements in the atomic number range $16 \leq Z \leq 92$ by photon impact at various energies. Atomic Data and Nuclear Data Tables, 159, 101662.

Amari, K., Kahoul, A., Sampaio, J.M., Kasri, Y., Daoudi, S., Marques, J.P., Parente, F., Hamidani, A., Croft, S., Favalli, A., Deghefel. B., Zidi, A., Berkani, B., 2024b. Empirical calculation of K-shell fluorescence cross sections for elements in the atomic range $16 \leq Z \leq 92$ by photon effects ranging from 5.46 to 123.6 keV (Three-dimensional formulae). Phys. Scr. 99, 105402.

Baydaş, E., Şahin, Y., Büyükkasap, E., 2003. Variation of K X-Ray Fluorescence Cross-Sections for Elements in the Range $22 \leq Z \leq 29$ at Various Energies. J. Trace Microprobe Tech. 21, 433–442.

Berger, M. J., Hubbell, J. H., Seltzer, S. M., Chang, J. 2010. Photon cross sections for materials of potential dosimetric interest. J. Appl. Phys. 58(10), 2333-2342.

Demir, D., Şahin, Y., 2013. Measurement of K X-ray fluorescence parameters in elements with $24 \leq Z \leq 65$ in an external magnetic field. Radiat. Phys. Chem. 85, 64–69.

Dogan, M., Aylikci, V., Tiraşoglu, E., Karahan, İ.H., 2014. Influence of pH and glycine on the K X-ray fluorescence parameters of Zn and Cr in Zn–Cr alloys. J. Radiat. Res. Appl. Sci. 7, 241–248.

Dogan, M., Tirasoglu, E., Karahan, İ.H., Kup Aylikci, N., Aylikci, V., Kahoul, A., Cetinkara, H.A., Serifoglu, O., 2013. Alloying effect on K X-ray intensity ratio and production cross section values of Zn and Cr in Zn-Cr alloys. Radiat. Phys. Chem. 87, 6–15.

Hubbell, J.H., Seltzer, S.M., 1995. Tables of x-ray mass attenuation coefficients and mass energy-absorption coefficients 1 keV to 20 MeV for elements Z = 1 to 92 and 48 additional substances of dosimetry interest (No. NIST IR 5632). National Institute of Standards and Technology, Gaithersburg, MD.

Krause, M.O., Nestor, C.W.Jr., Sparks, C.J.Jr., Ricci, E., 1978. X-ray fluorescence cross sections for K and L x rays of the elements (No. ORNL-5399, 7032250) Oak. Ridge.National.Lab.

Puri, S., Chand, B., Mehta, D., Garg, M.L., Singh, N., Trehan, P.N., 1995. K and L Shell X-Ray Fluorescence Cross Sections. At. Data Nucl. Data Tables 61, 289–311.

Rao, D.V., Cesareo, R., Gigante, G.E., 1993. K X-ray fluorescence cross-sections for some light elements excited by keV photons. Appl. Phys. Solids Surf. 56, 401–403.

Scofield, J. H. 1973. Theoretical photoionization cross sections from 1 to 1500 keV (No. UCRL-51326). California Univ., Livermore. Lawrence Livermore Lab.

Seven, S., 2012. Energy dependence of photon-induced Kα and Kβ x-ray production cross-sections for some elements with 38≤Z≤51 in the energy range 20–50keV. Radiat. Phys. Chem. 81, 489–494

Seven, S., Erdoğan, H., 2015. Energy dependence of photon-induced Kα and Kβ x-ray production cross-sections for some elements with 42≤ Z≤ 68 in the energy range 38–80 keV. Radiat. Phys. Chem. 117, 1–6.

Singh, S., Rani, R., Mehta, D., Singh, N., Mangal, P.C., Trehan, P.N., 1990. K x-ray fluorescence cross-section measurements of some elements in the energy range 8-47 keV. X-Ray Spectrom. 19, 155–158.

Turhan, M.F., Akman, F., 2023. K-shell fluorescence parameters of some elements at 59.54 keV: Experimental and theoretical results. Nucl. Instrum. Methods Phys. Res. Sect. B Beam Interact. Mater. At. 534, 16–25.

Uğurlu, M., Demir, L., 2020. *K* X-ray fluorescence parameters of some fourth period elements in a magnetic field. Spectrosc. Lett. 53, 163–171.

Fig. 1

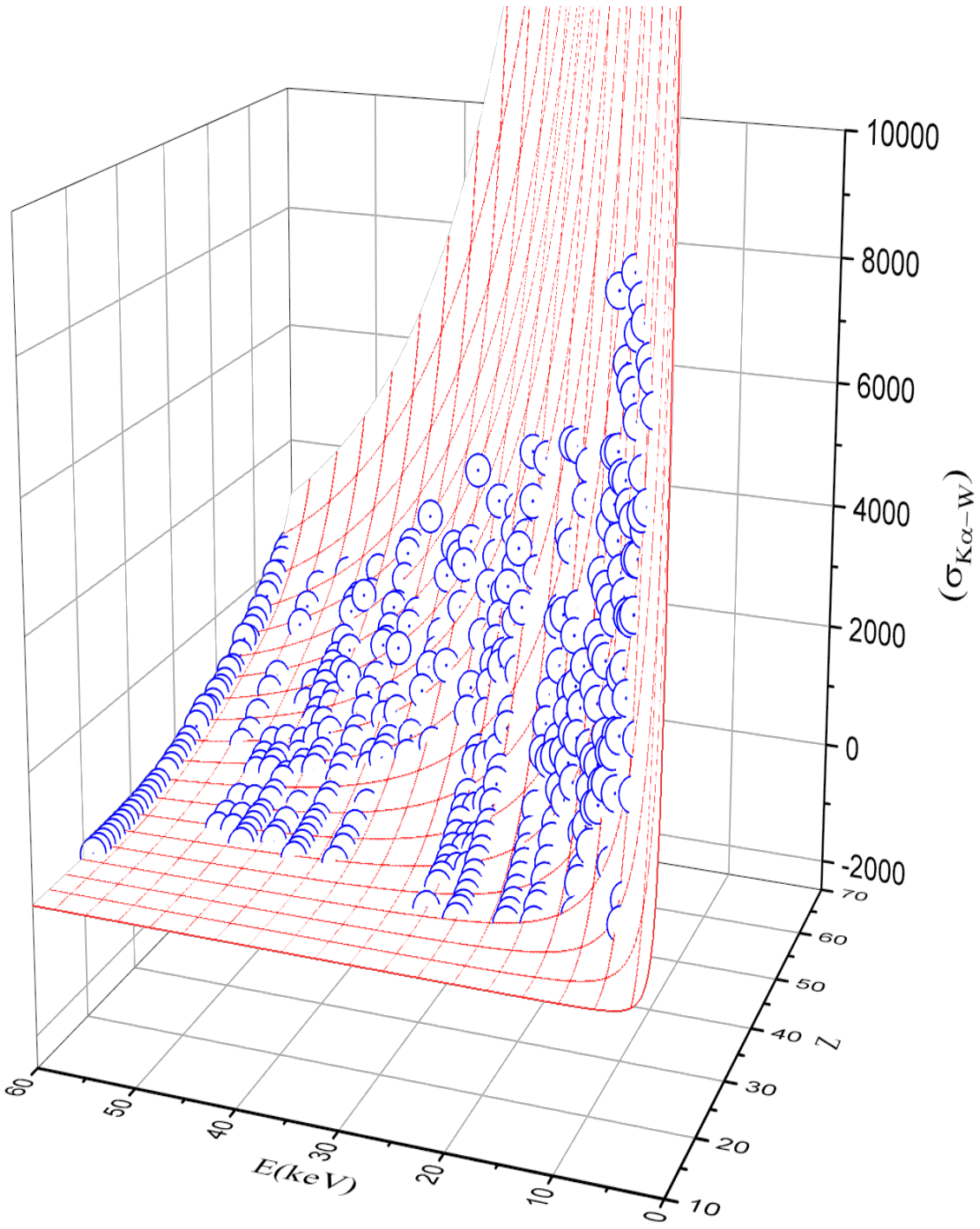
10000
8000
6000
4000
2000
0
-2000
$(\sigma_{K\alpha-W})$
70
60
50
40
30
20
10
Z
60
50
40
30
20
10
0
E(keV)

Fig. 2

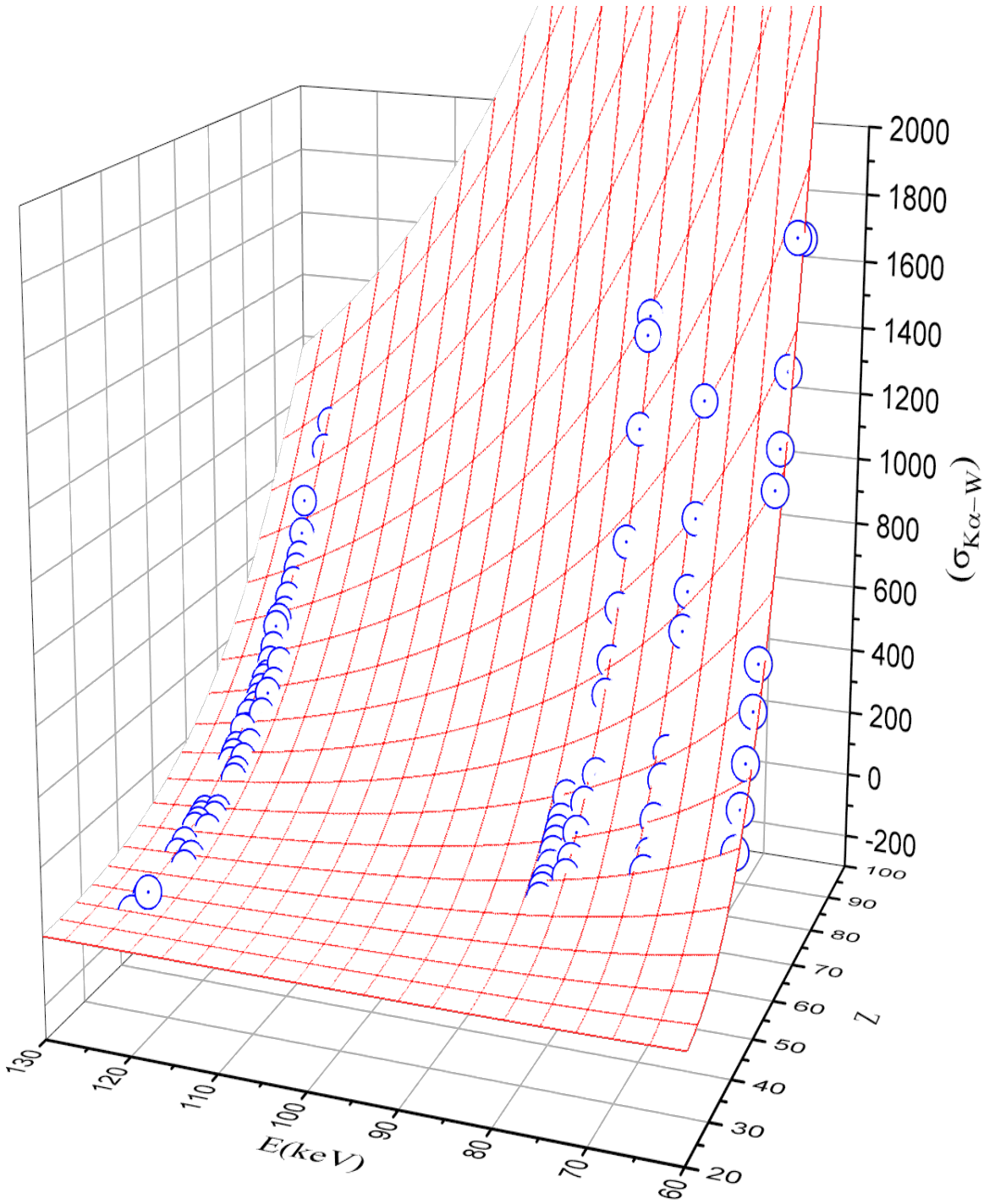
2000
1800
1600
1400
1200
1000
800
600
400
200
0
-200
$(\sigma_{K\alpha-W})$
130
120
110
100
90
80
70
60
E(keV)
100
90
80
70
60
50
40
30
20
Z

Fig. 3

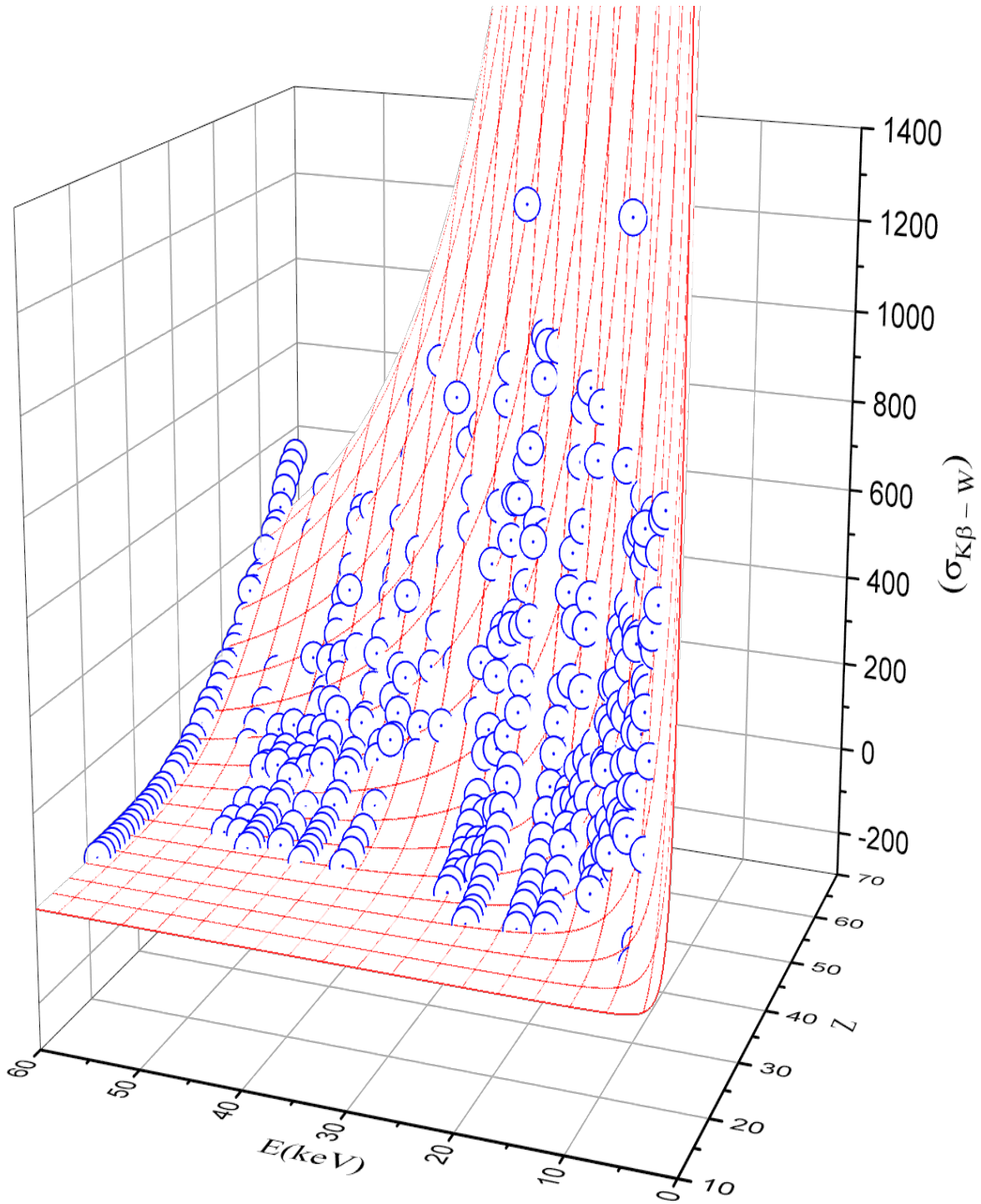
1400
1200
1000
800
600
400
200
0
-200
$(\sigma_{K\beta-W})$
70
60
50
40
Z
30
20
10
60
50
40
30
20
10
0
E(keV)

Fig. 4

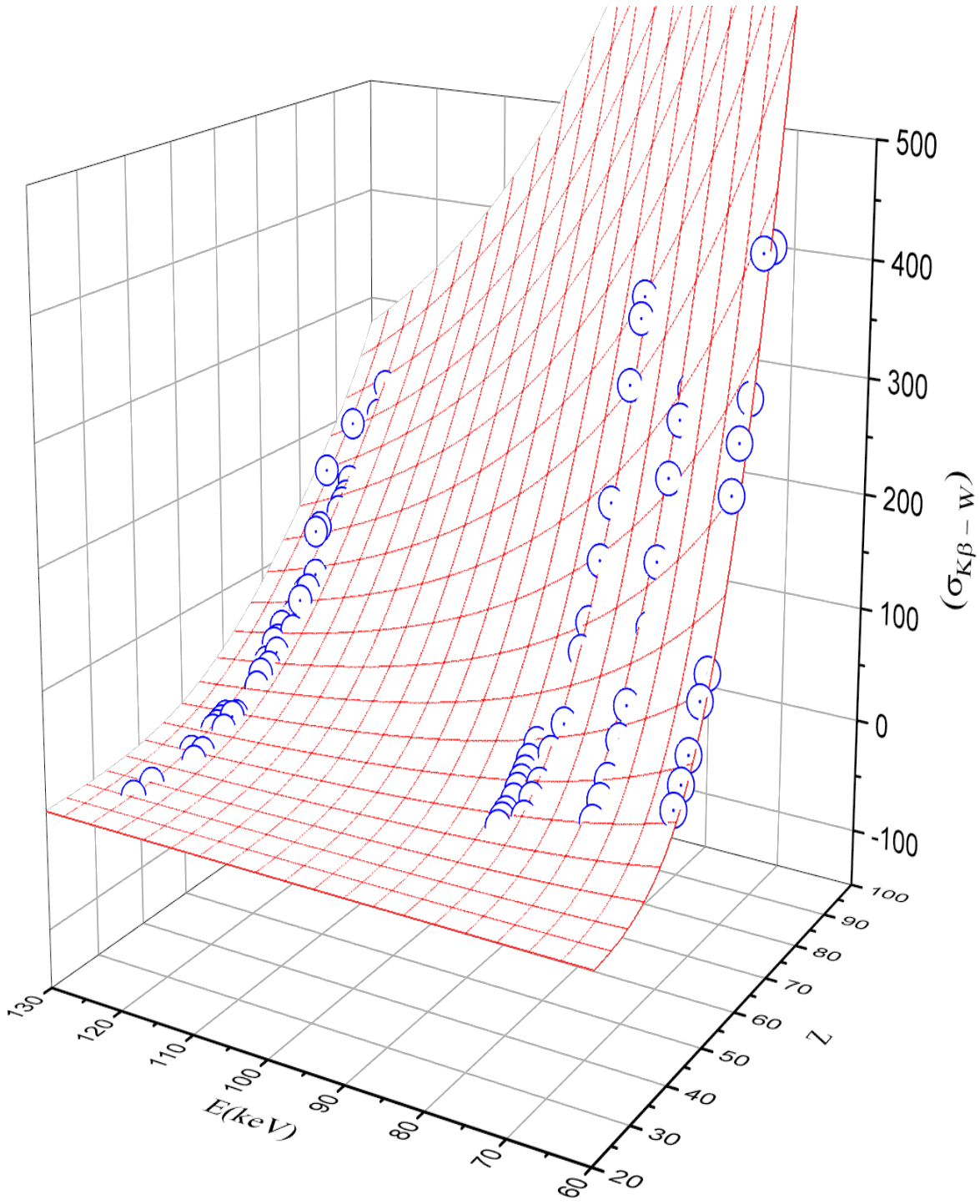
500
400
300
200
100
0
-100
$(\sigma_{K\beta-W})$
130
120
110
100
90
80
70
60
E(keV)
100
90
80
70
60
50
40
30
20
Z

Fig. 5

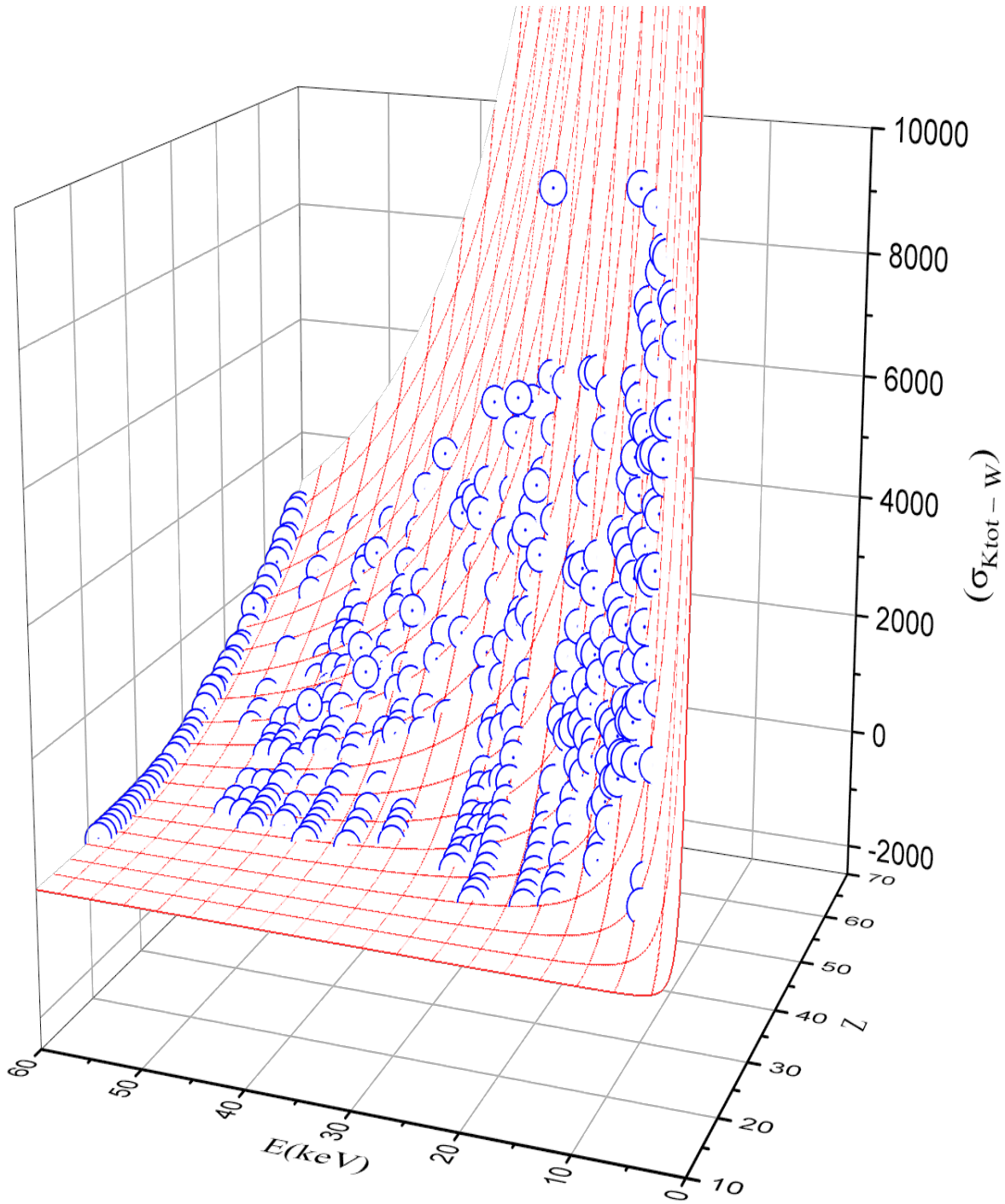
10000
8000
6000
4000
2000
0
-2000
$(\sigma_{Ktot} - W)$
70
60
50
40
30
20
10
Z
60
50
40
30
20
10
0
E(keV)

Fig. 6

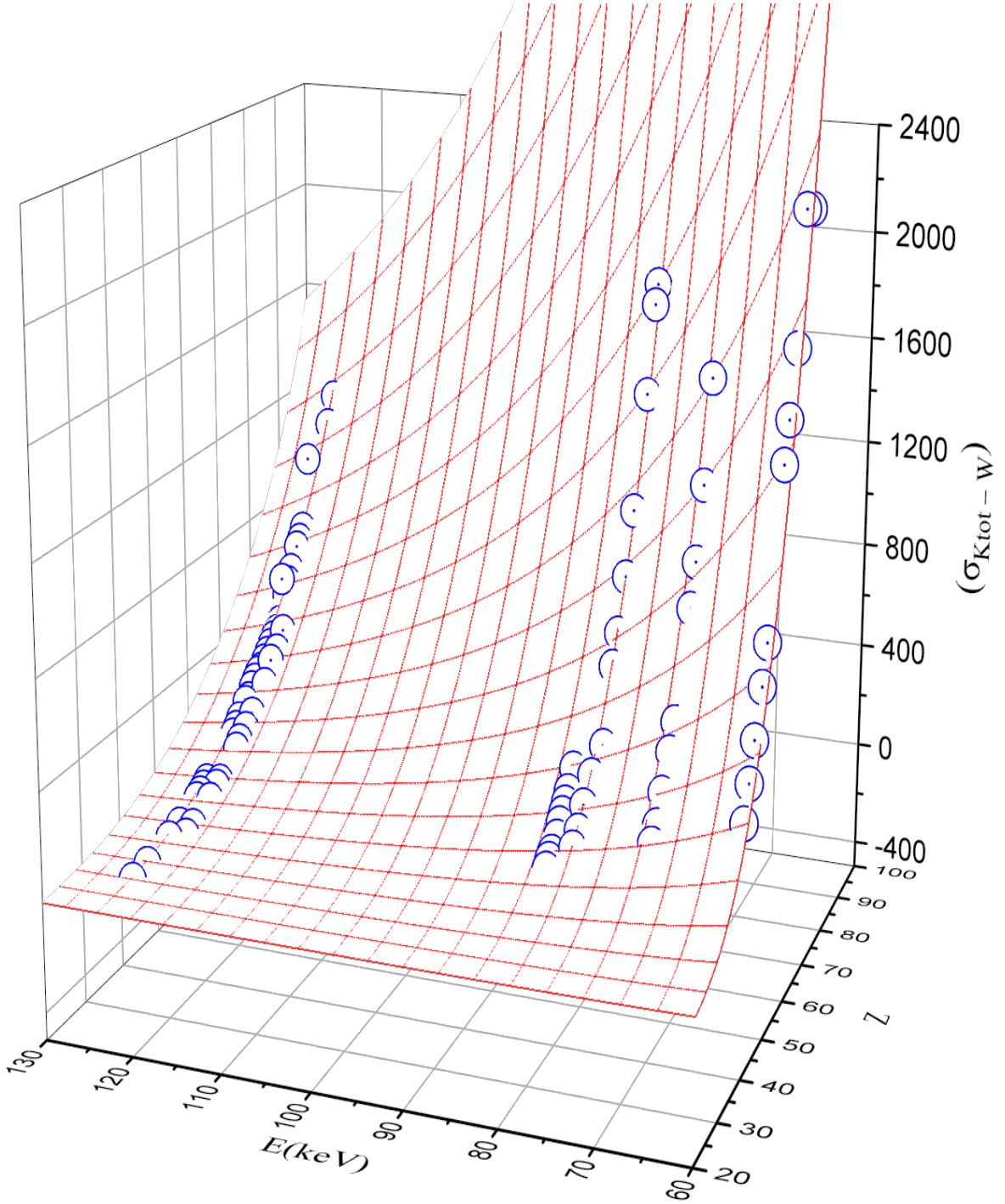
2400
2000
1600
1200
800
400
0
-400
$(\sigma_{Ktot} - W)$
100
90
80
70
60
50
40
30
20
Z
130
120
110
100
90
80
70
60
E(keV)

Fig. 7

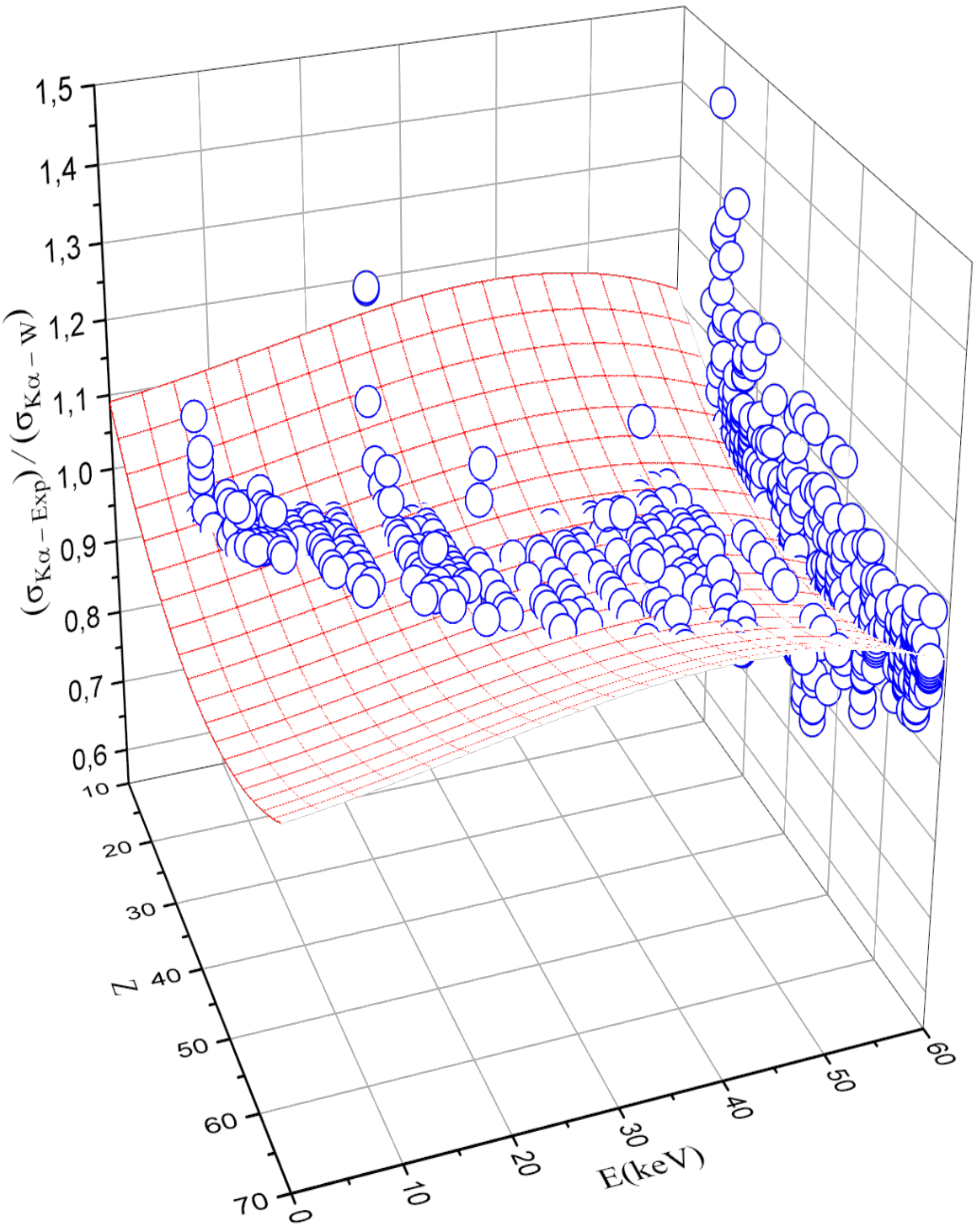
1,5
1,4
1,3
1,2
1,1
1,0
0,9
0,8
0,7
0,6
$(\sigma_{K\alpha-Exp})/(\sigma_{K\alpha-W})$
10
20
30
Z 40
50
60
70
0
10
20
30
40
50
60
E(keV)

Fig. 8

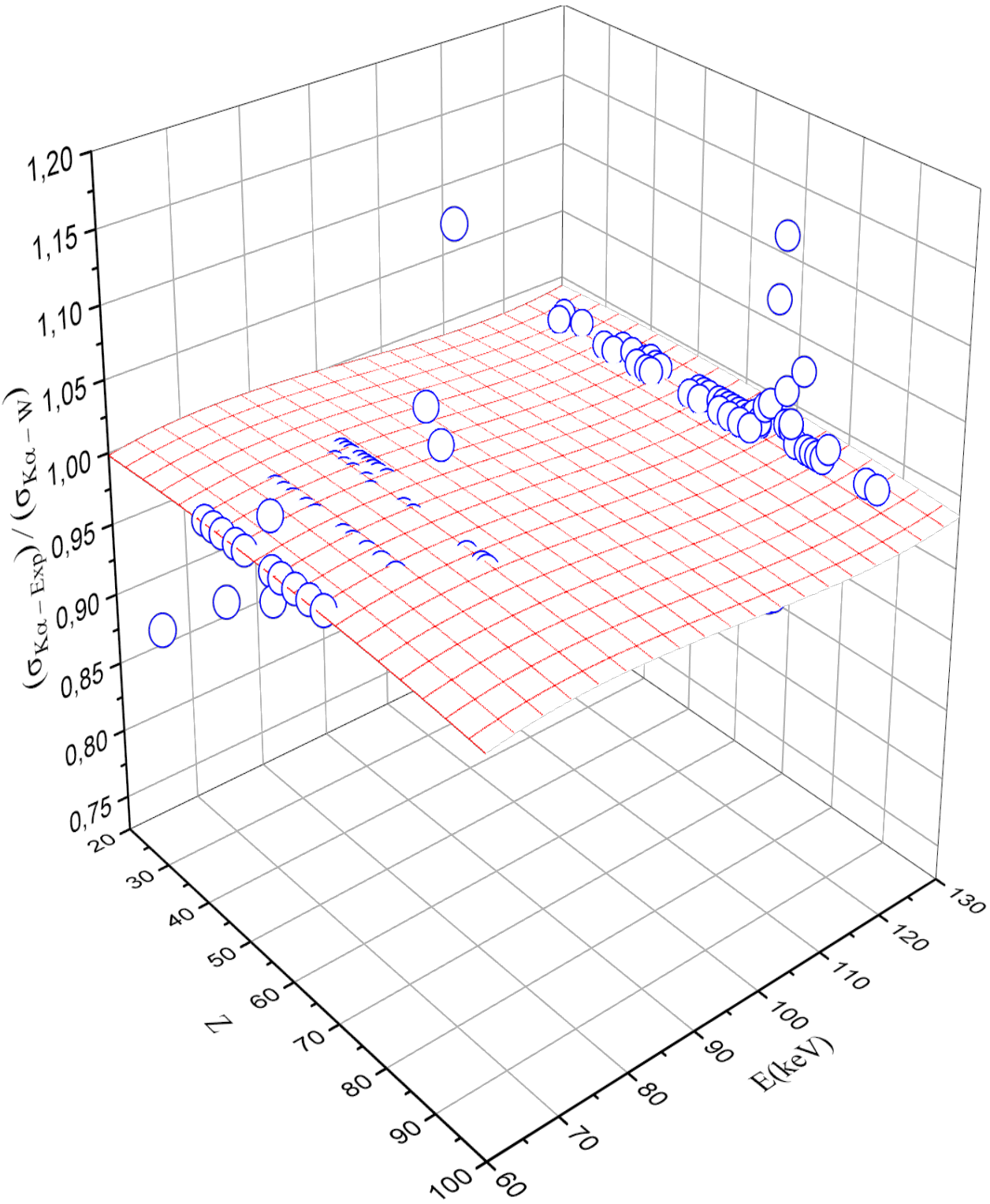
1,20
1,15
1,10
1,05
1,00
0,95
0,90
0,85
0,80
0,75
$(\sigma_{K\alpha-Exp}) / (\sigma_{K\alpha-W})$
20
30
40
50
60
70
80
90
100
Z
60
70
80
90
100
110
120
130
E(keV)

Fig. 9

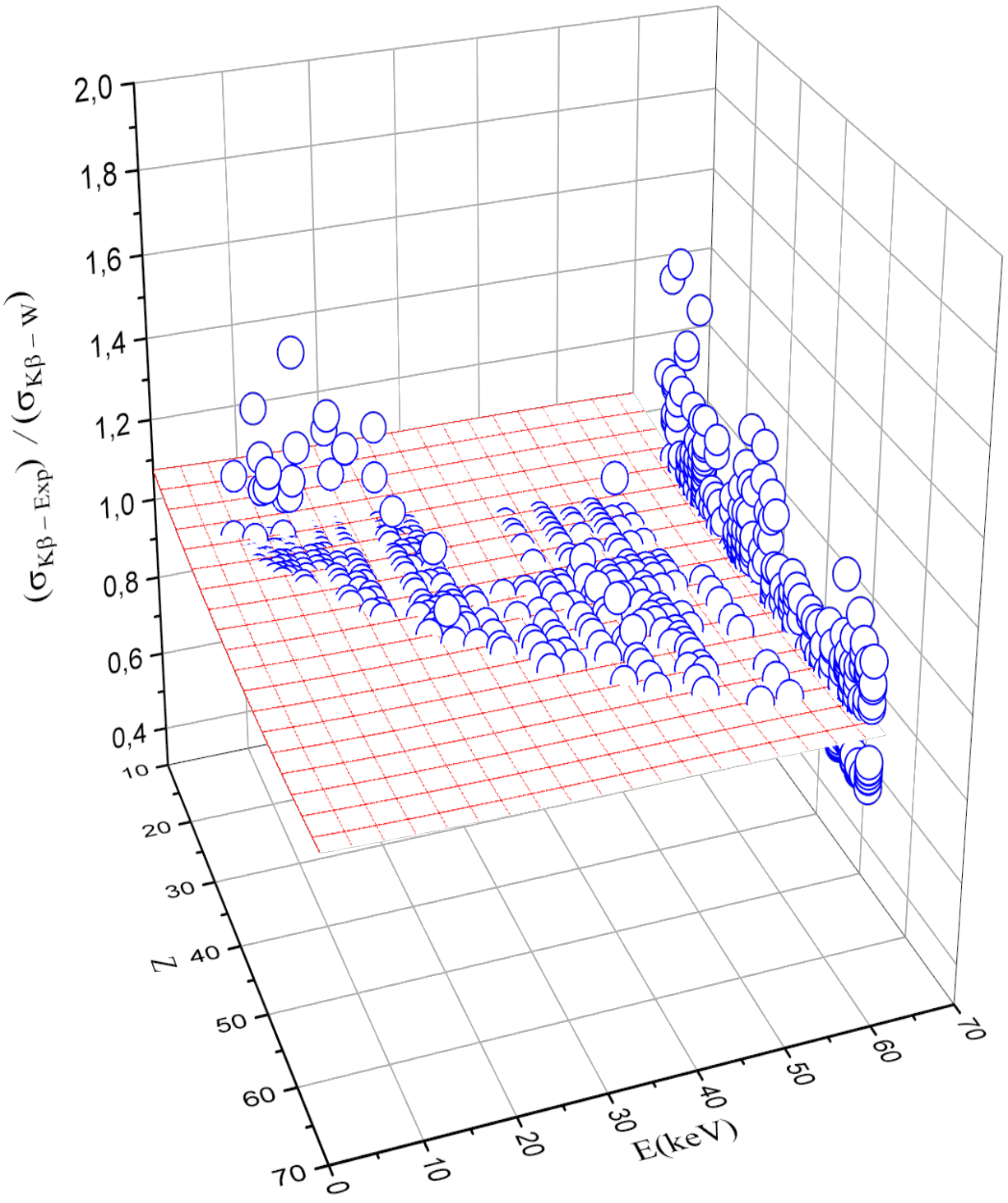
2,0
1,8
1,6
1,4
1,2
1,0
0,8
0,6
0,4
$(\sigma_{K\beta-Exp}) / (\sigma_{K\beta-W})$
10
20
30
Z 40
50
60
70
0
10
20
30
40
50
60
70
E(keV)

Fig. 10

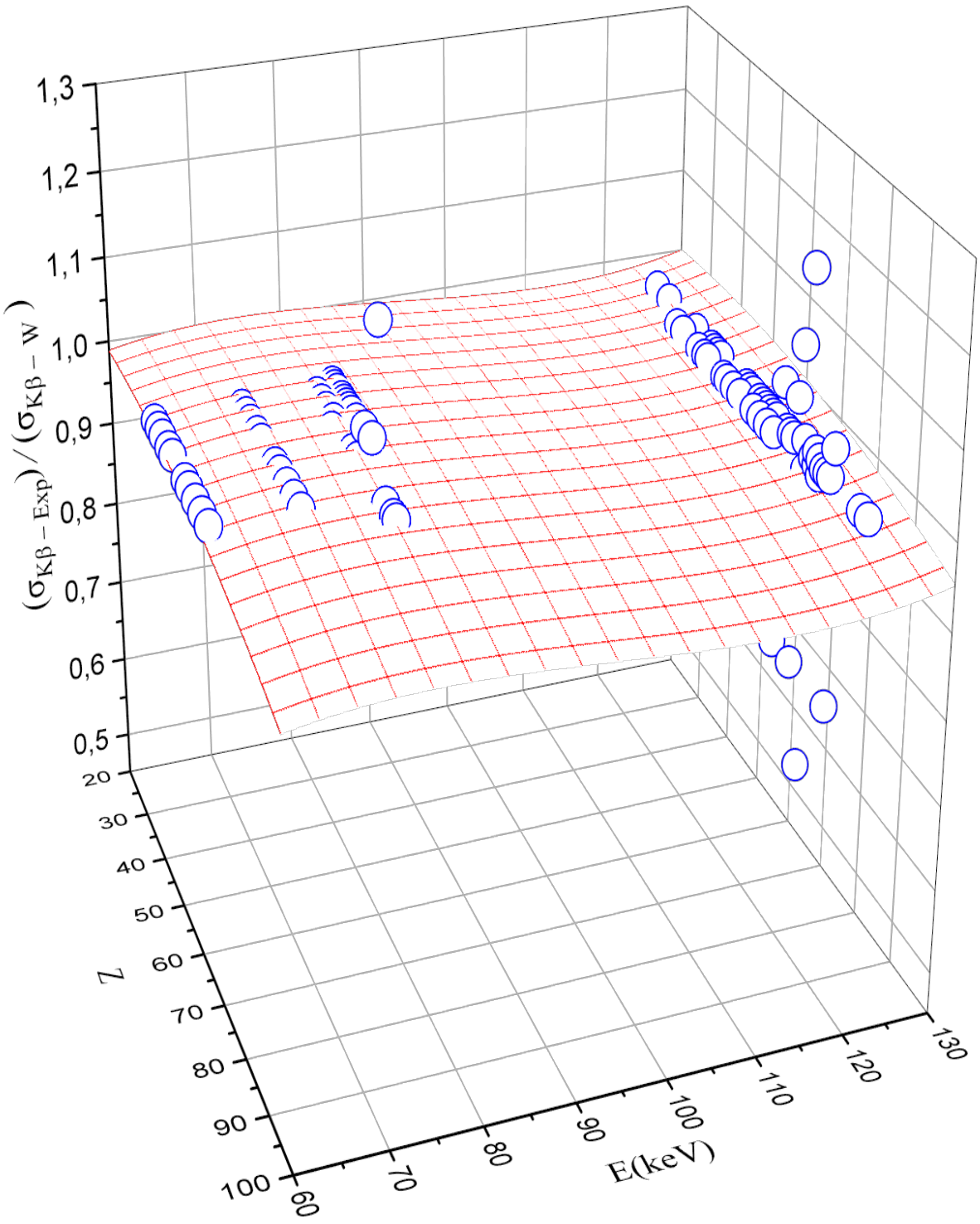
1,3
1,2
1,1
1,0
0,9
0,8
0,7
0,6
0,5
(σKβ – Exp) / (σKβ – W)
20
30
40
50
60
70
80
90
100
Z
60
70
80
90
100
110
120
130
E(keV)

Fig. 11

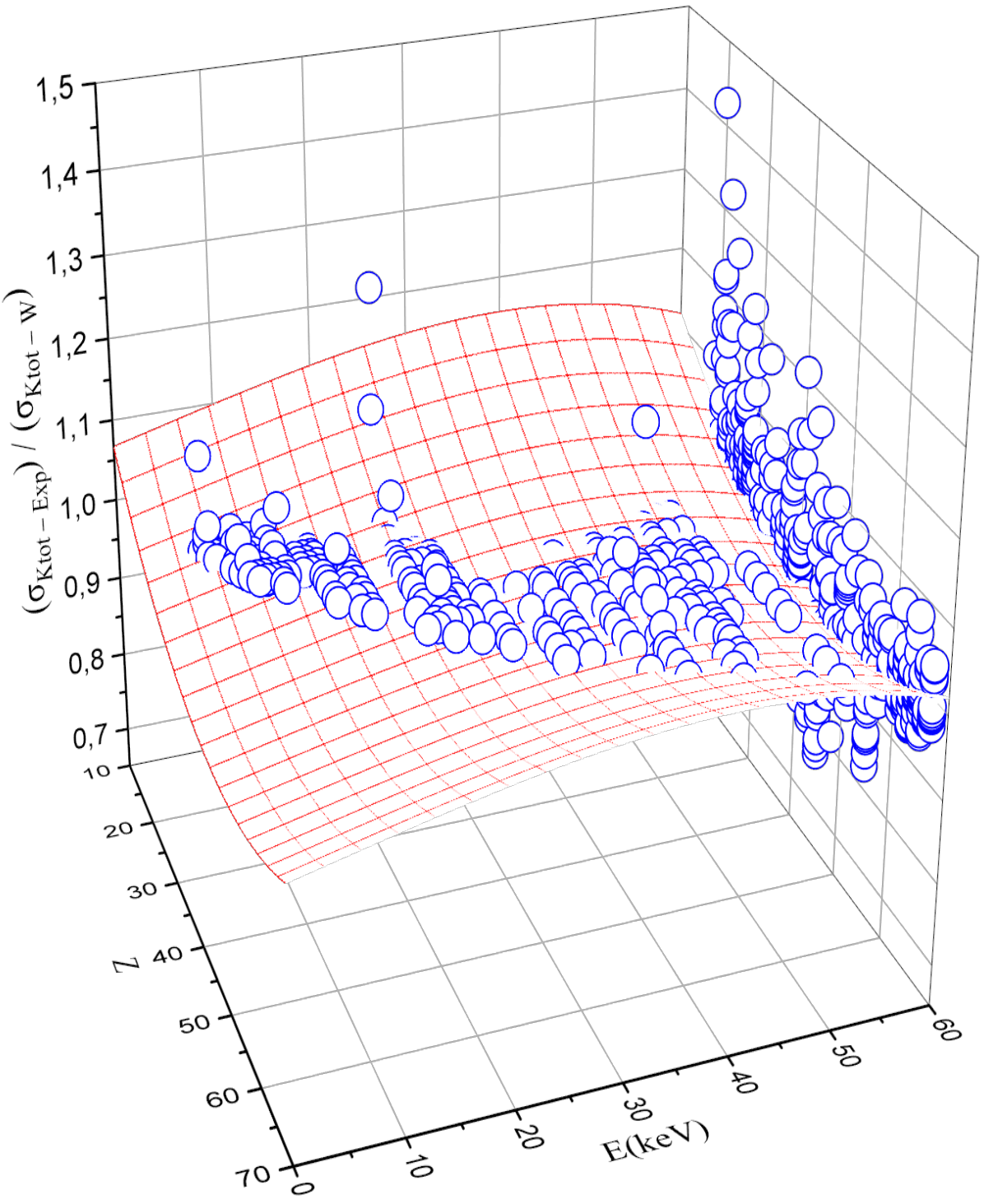
1,5
1,4
1,3
1,2
1,1
1,0
0,9
0,8
0,7
(σKtot – Exp) / (σKtot – W)
10
20
30
Z 40
50
60
70
0
10
20
30
40
50
60
E(keV)

Fig. 12

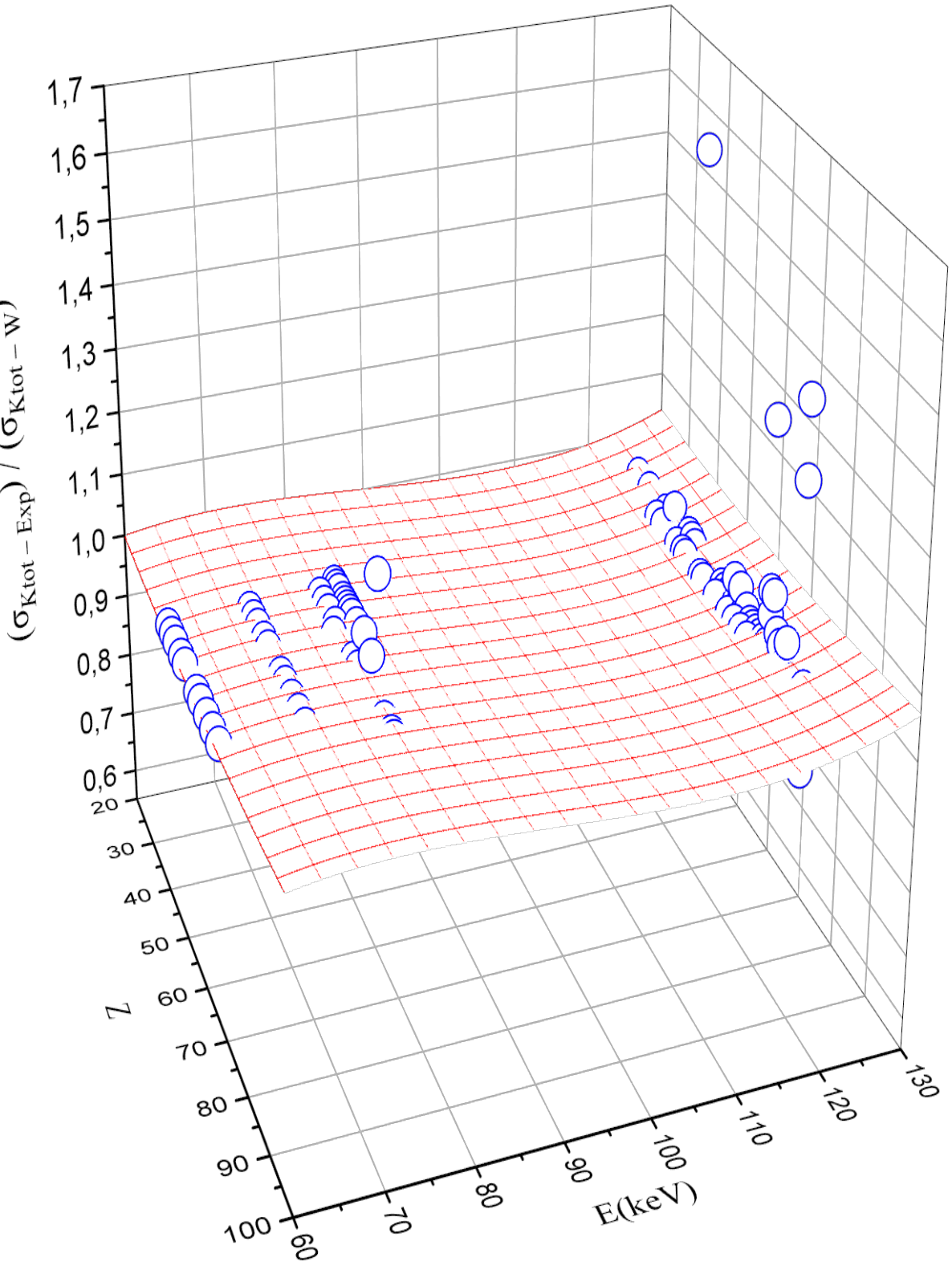
(σKtot – Exp) / (σKtot – W)
1,7
1,6
1,5
1,4
1,3
1,2
1,1
1,0
0,9
0,8
0,7
0,6
Z
20
30
40
50
60
70
80
90
100
E(keV)
60
70
80
90
100
110
120
130

Fig. 13

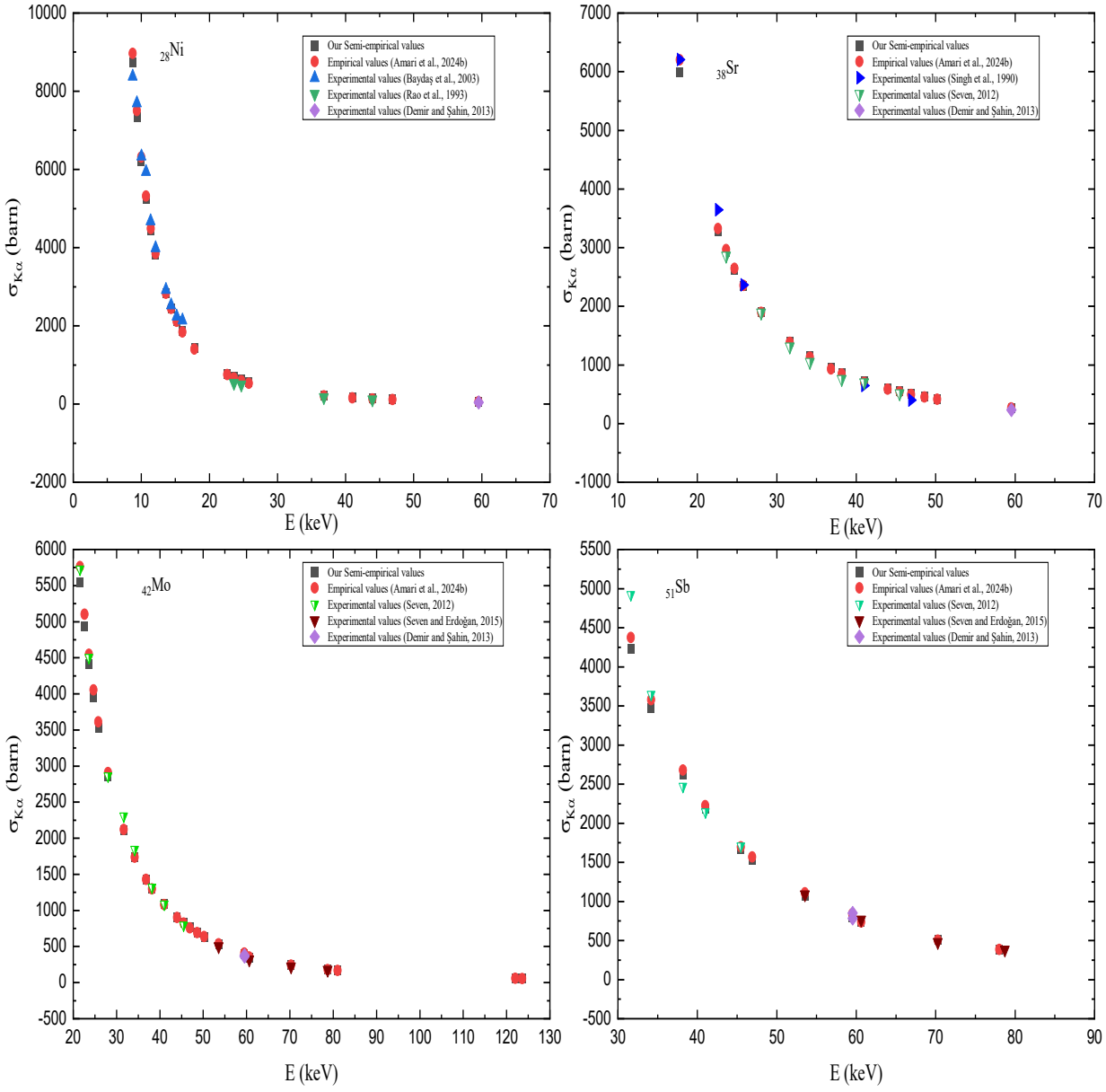
$_{28}$Ni
Our Semi-empirical values
Empirical values (Amari et al., 2024b)
Experimental values (Baydaş et al., 2003)
Experimental values (Rao et al., 1993)
Experimental values (Demir and Şahin, 2013)
$_{38}$Sr
Our Semi-empirical values
Empirical values (Amari et al., 2024b)
Experimental values (Singh et al., 1990)
Experimental values (Seven, 2012)
Experimental values (Demir and Şahin, 2013)
$_{42}$Mo
Our Semi-empirical values
Empirical values (Amari et al., 2024b)
Experimental values (Seven, 2012)
Experimental values (Seven and Erdoğan, 2015)
Experimental values (Demir and Şahin, 2013)
$_{51}$Sb
Our Semi-empirical values
Empirical values (Amari et al., 2024b)
Experimental values (Seven, 2012)
Experimental values (Seven and Erdoğan, 2015)
Experimental values (Demir and Şahin, 2013)
$\sigma_{K\alpha}$ (barn)
E (keV)

Fig. 14

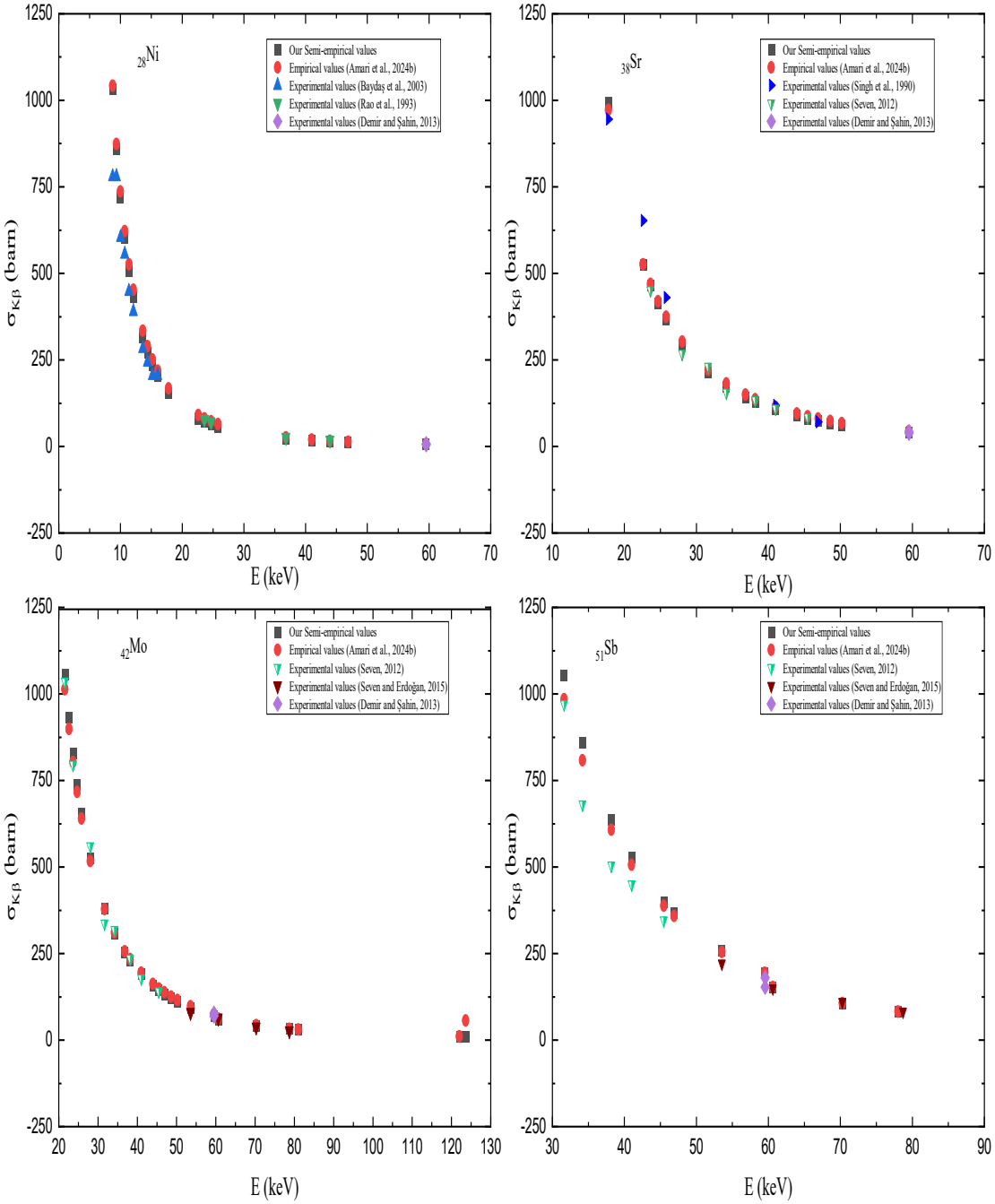
28Ni
Our Semi-empirical values
Empirical values (Amari et al., 2024b)
Experimental values (Baydaş et al., 2003)
Experimental values (Rao et al., 1993)
Experimental values (Demir and Şahin, 2013)
38Sr
Our Semi-empirical values
Empirical values (Amari et al., 2024b)
Experimental values (Singh et al., 1990)
Experimental values (Seven, 2012)
Experimental values (Demir and Şahin, 2013)
42Mo
Our Semi-empirical values
Empirical values (Amari et al., 2024b)
Experimental values (Seven, 2012)
Experimental values (Seven and Erdoğan, 2015)
Experimental values (Demir and Şahin, 2013)
51Sb
Our Semi-empirical values
Empirical values (Amari et al., 2024b)
Experimental values (Seven, 2012)
Experimental values (Seven and Erdoğan, 2015)
Experimental values (Demir and Şahin, 2013)
σKβ (barn)
E (keV)

Fig. 15

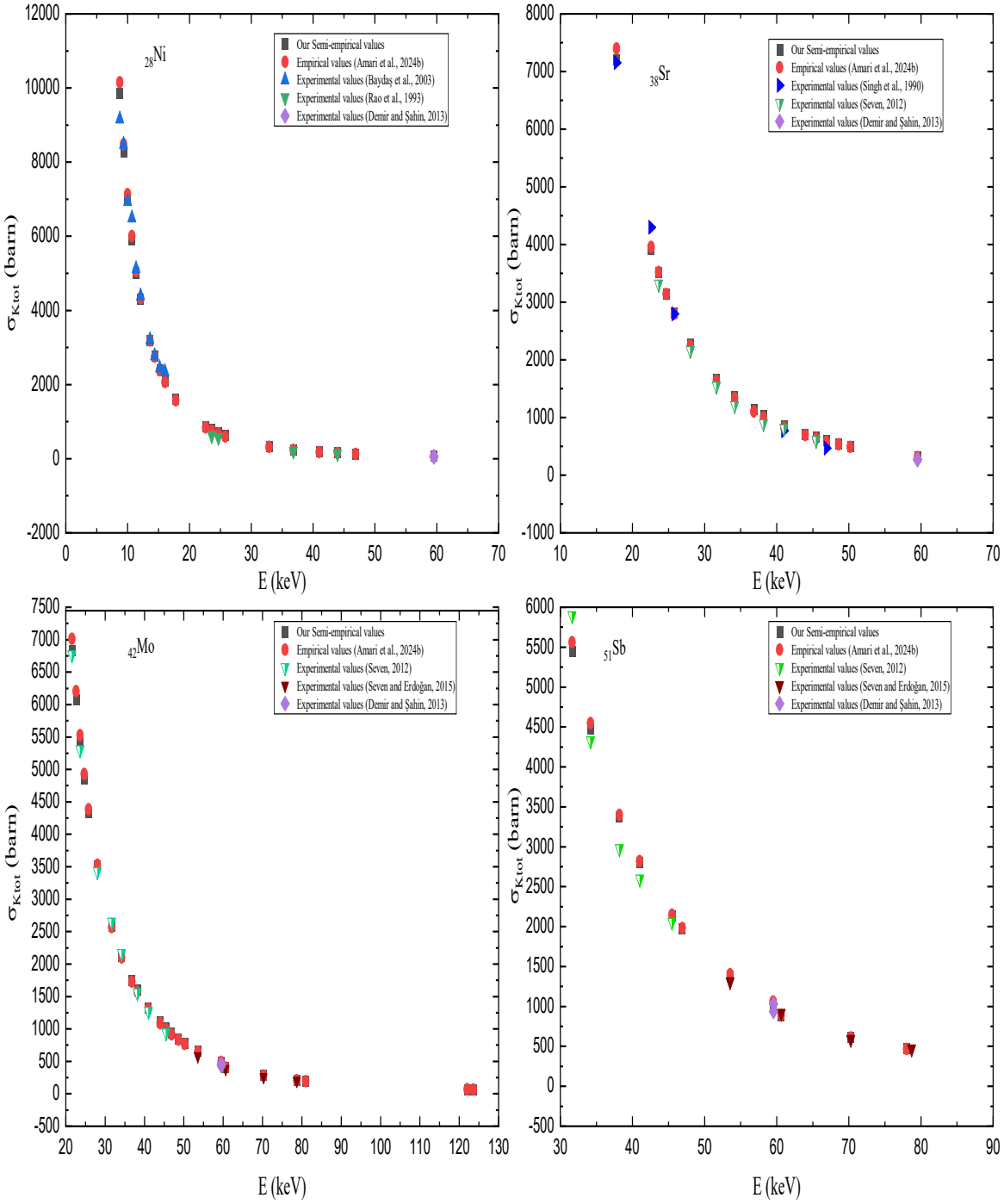
$_{28}$Ni
Our Semi-empirical values
Empirical values (Amari et al., 2024b)
Experimental values (Baydaş et al., 2003)
Experimental values (Rao et al., 1993)
Experimental values (Demir and Şahin, 2013)
σ_{Ktot} (barn)
E (keV)
$_{38}$Sr
Our Semi-empirical values
Empirical values (Amari et al., 2024b)
Experimental values (Singh et al., 1990)
Experimental values (Seven, 2012)
Experimental values (Demir and Şahin, 2013)
σ_{Ktot} (barn)
E (keV)
$_{42}$Mo
Our Semi-empirical values
Empirical values (Amari et al., 2024b)
Experimental values (Seven, 2012)
Experimental values (Seven and Erdoğan, 2015)
Experimental values (Demir and Şahin, 2013)
σ_{Ktot} (barn)
E (keV)
$_{51}$Sb
Our Semi-empirical values
Empirical values (Amari et al., 2024b)
Experimental values (Seven, 2012)
Experimental values (Seven and Erdoğan, 2015)
Experimental values (Demir and Şahin, 2013)
σ_{Ktot} (barn)
E (keV)

Table 1. The fitting coefficients for the calculation of the semi-empirical K_α, K_β and K_{tot} XRF cross section for photon energy range according to the formulae (1) and (3). The associated root-mean-square errors (ε_{rms}) are also included.

	Z-range	**E-range (keV)**		a_n, b_i, l_j, c	**Values**	ε_{rms}**(%)**
σ_{K_α}	$16 \le Z \le 68$	$5.46 \le E \le 59.5$	$f(Z)$	a_0	-3.25239	19.10
				a_1	0.503749	
				a_2	-0.012183	
				a_3	0.0000853352	
			$g(Z,E)$	c	0.0432218	
				d	2.5732	
			$P(Z)$	b_0	1.80376	
				b_1	-0.0182378	
				b_2	0.000202691	
			$Q(E)$	l_0	0.664442	
				l_1	0.00097383	
				l_2	0.0000421914	
				l_3	-0.000000906032	
	$29 \le Z \le 92$	$59.5 \le E \le 123.6$	$f(Z)$	a_0	18828.9	29.50
				a_1	-453.785	
				a_2	4.36452	
				a_3	-0.0151818	
			$g(Z,E)$	c	0.0000143745	
				d	2.54167	
			$P(Z)$	b_0	0.612071	
				b_1	0.00023402	
				b_2	-0.00000240025	
			$Q(E)$	l_0	1.15628	
				l_1	0.0161208	
				l_2	-0.000176084	
				l_3	0.000000608389	
σ_{K_β}	$16 \le Z \le 68$	$5.46 \le E \le 59.5$	$f(Z)$	a_0	1.0085	5.73
				a_1	1.13416	
				a_2	0.796068	
				a_3	-0.0109203	
			$g(Z,E)$	c	0.0000461029	
				d	2.67242	
			$P(Z)$	b_0	1.48984	
				b_1	-0.00534623	

				b_2	0.0000511364	
			$Q(E)$	l_0	0.745043	
				l_1	-0.000652673	
				l_2	0.0000177804	
				l_3	-0.000000176022	
	$29 \leq Z \leq 92$	$59.5 \leq E \leq 123.6$	$f(Z)$	a_0	584.29	14.03
				a_1	1691.82	
				a_2	$-$ 28.7889	
				a_3	0.130059	
			$g(Z,E)$	c	0.000000348419	
				d	2.44892	
			$P(Z)$	b_0	0.320062	
				b_1	0.000450297	
				b_2	-0.00000532314	
			$Q(Z)$	l_0	1.02809	
				l_1	0.0697641	
				l_2	-0.00077259	
				l_3	0.00000273862	
$\boldsymbol{\sigma_{K_{tot}}}$	$16 \leq Z \leq 68$	$5.46 \leq E \leq 59.5$	$f(Z)$	a_0	-4.29442	97.59
				a_1	0.586237	
				a_2	$-$ 0.0130736	
				a_3	0.000084683	
			$g(Z,E)$	c	0.0426787	
				d	2.58517	
			$P(Z)$	b_0	0.922452	
				b_1	-0.00842489	
				b_2	0.000090228	
			$Q(Z)$	l_0	1.25954	
				l_1	0.00368367	
				l_2	0.0000114867	
				l_3	-0.000000950401	
	$29 \leq Z \leq 92$	$59.5 \leq E \leq 123.6$	$f(Z)$	a_0	15409	12.61
				a_1	-246.884	
				a_2	1.18599	
				a_3	-0.000127354	
			$g(Z,E)$	c	0.0000154721	
				d	2.55095	
			$P(Z)$	b_0	0.200262	

		b_1	-0.000196012
		b_2	0.00000230659
	$Q(Z)$	l_0	0.962254
		l_1	0.148344
		l_2	-0.00171436
		l_3	0.00000636515

Table 2. Comparison of se-empirical K_α X-ray fluorescence cross-section (in barn) deduced from this work by photon impact with the experimental values in the literature and with empirical values of Amari *et al.* (2024b).

E(KeV)	Our results			Other Experimentales works				
		Empirical values		Experimentales Values				
	Semi-empirical values	Amari *et al.* (2024b)	Baydaş *et al.* (2003)	Rao *et al*. (1993)	Demir and Şahin (2013)	Singh *et al.* (1990)	Seven (2012)	Seven and Erdoğan (2015)
$_{28}$Ni								
8.74	8751.79	8971.26	8382	-	-	-	-	-
9.36	7347.01	7502.16	7699	-	-	-	-	-
10	6206.23	6312.97	6335	-	-	-	-	-
10.68	5247.91	5317.16	5945	-	-	-	-	-
11.4	4444.3	4484.83	4678	-	-	-	-	-
12.09	3826.76	3847.25	3996	-	-	-	-	-
13.6	2836.97	2829.94	2924	-	-	-	-	-
14.38	2462.27	2446.68	2534	-	-	-	-	-
15.2	2138.98	2117.05	2242	-	-	-	-	-
16.04	1866.21	1839.81	2144	-	-	-	-	-
17.8	1433.55	1402.13	-	-	-	-	-	-
22.6	783.97	752.01	-	-	-	-	-	-
23.62	701.3	670.19	-	538	-	-	-	-
24.68	627.74	597.65	-	496	-	-	-	-
25.8	561.22	532.3	-	-	-	-	-	-
36.82	227.99	210.42	-	173	-	-	-	-
41	173.02	158.94	-	-	-	-	-	-
43.95	144.49	132.59	-	116	-	-	-	-
46.9	121.84	111.91	-	-	-	-	-	-
59.5	63.39	60.15	-	-	46.35	-	-	-
$_{38}$Sr								
17.8	5989.08	6203.41	-	-	-	6207	-	-
22.6	3275.28	3327.1	-	-	-	3644	-	-
23.62	2929.88	2965.1	-	-	-	-	2861.99	-
24.68	2622.59	2644.18	-	-	-	-	-	-
25.8	2344.68	2355.03	-	-	-	2364	-	-
28.03	1901.93	1896.92	-	-	-	-	1892.96	-
31.64	1400.17	1382.8	-	-	-	-	1311.54	-
34.17	1152.03	1131.31	-	-	-	-	1048.47	-
36.82	952.51	930.97	-	-	-	-	-	-
38.18	868.15	846.9	-	-	-	-	759.37	-
41	722.86	703.2	-	-	-	651	698.96	-
43.95	603.64	586.6	-	-	-	-	-	-
45.47	552.26	536.8	-	-	-	-	516.38	-
46.9	509.02	495.13	-	-	-	398	-	-
48.6	463.12	451.2	-	-	-	-	-	-
50.2	424.65	414.63	-	-	-	-	-	-
59.5	264.83	266.1	-	-	233.44	-	-	-
$_{42}$Mo								
21.57	5548.38	5764.14	-	-	-	-	5730.02	-

22.6	4931.83	5103.55	-	-	-	-	-	-
23.62	4411.74	4548.28	-	-	-	-	4506.6	-
24.68	3949.02	4056	-	-	-	-	-	-
25.8	3530.56	3612.46	-	-	-	-	-	-
28.03	2863.88	2909.75	-	-	-	-	2862.62	-
31.64	2108.34	2121.13	-	-	-	-	2308.26	-
34.17	1734.69	1735.36	-	-	-	-	1844.69	-
36.82	1434.26	1428.05	-	-	-	-	-	-
38.18	1307.24	1299.09	-	-	-	-	1320.12	-
41	1088.46	1078.66	-	-	-	-	1088.97	-
43.95	908.95	899.8	-	-	-	-	-	-
45.47	831.58	823.41	-	-	-	-	796.5	-
46.9	766.46	759.5	-	-	-	-	-	-
48.6	697.36	692.11	-	-	-	-	-	-
50.2	639.42	636.01	-	-	-	-	-	-
53.54	536.71	537.61	-	-	-	-	-	501.8
59.5	398.77	408.19	-	-	378.21	-	-	-
60.62	351.74	352.43	-	-	-	-	-	319.39
70.27	242.95	241.35	-	-	-	-	-	223.03
78.71	182.09	180.42	-	-	-	-	-	175.23
$_{51}$Sb								
31.64	4228.17	4374.73	-	-	-	-	4921.55	-
34.17	3478.83	3579.11	-	-	-	-	3645.67	-
38.18	2621.61	2679.33	-	-	-	-	2470.88	-
41	2182.84	2224.69	-	-	-	-	2145.34	-
45.47	1667.7	1698.25	-	-	-	-	1707.58	-
46.9	1537.1	1566.43	-	-	-	-	-	-
53.54	1076.35	1108.81	-	-	-	-	-	1087.63
59.5	799.72	841.87	-	-	764.32	-	-	-
60.62	735.49	737.2	-	-	-	-	-	764.32
70.27	508.01	504.84	-	-	-	-	-	479.21
78.01	389.61	386.2	-	-	-	-	-	383.37

Table 3. Comparison of semi-empirical K_β X-ray fluorescence cross-section (in barn) deduced from this work by photon impact with the experimental values literature and with empirical values of Amari *et al.* (2024b).

E(KeV)	**Our results**		**Other Experimentales works**					
		Empirical values		Experimentales Values				
	Semi-empirical values	Amari *et al.* (2024b)	Baydaş *et al.* (2003)	Rao *et al*. (1993)	Demir and Şahin (2013)	Singh *et al.* (1990)	Seven (2012)	Seven and Erdoğan (2015)
$_{28}$Ni								
8.74	1030.94	1041.67	780	-	-	-	-	-
9.36	858.13	873.38	780	-	-	-	-	-
10	718.88	736.81	604	-	-	-	-	-
10.68	602.79	622.15	556	-	-	-	-	-
11.4	506.18	526.08	448	-	-	-	-	-
12.09	432.49	452.3	390	-	-	-	-	-
13.6	315.6	334.21	283	-	-	-	-	-
14.38	271.83	289.57	244	-	-	-	-	-
15.2	234.32	251.09	205	-	-	-	-	-
16.04	202.89	218.66	205	-	-	-	-	-
17.8	153.54	167.31	-	-	-	-	-	-
22.6	81.04	90.56	-	-	-	-	-	-
23.62	72.01	80.84	-	78	-	-	-	-
24.68	64.03	72.21	-	71	-	-	-	-
25.8	56.86	64.43	-	-	-	-	-	-
36.82	21.96	25.82	-	26	-	-	-	-
41	16.47	19.58	-	-	-	-	-	-
43.95	13.67	16.38	-	18	-	-	-	-
46.9	11.49	13.86	-	-	-	-	-	-
59.5	6.05	7.52	-	-	7.51	-	-	-
$_{38}$Sr								
17.8	992.86	972.03	-	-	-	945	-	-
22.6	524.04	526.13	-	-	-	652	-	-
23.62	465.65	469.68	-	-	-	-	451.78	-
24.68	414.04	419.55	-	-	-	-	-	-
25.8	367.68	374.31	-	-	-	430	-	-
28.03	294.55	302.45	-	-	-	-	268.01	-
31.64	213.02	221.51	-	-	-	-	230.33	-
34.17	173.4	181.76	-	-	-	-	156.12	-
36.82	142	150	-	-	-	-	-	-
38.18	128.86	136.64	-	-	-	-	133.57	-
41	106.49	113.77	-	-	-	118	108.98	-
43.95	88.41	95.16	-	-	-	-	-	-
45.47	80.71	87.19	-	-	-	-	84.54	-
46.9	74.28	80.52	-	-	-	71	-	-
48.6	67.51	73.48	-	-	-	-	-	-
50.2	61.89	67.6	-	-	-	-	-	-
59.5	39.15	43.67	-	-	42.03	-	-	-

$_{42}$Mo								
21.57	1056.8	1013.53	-	-	-	-	1035.77	-
22.6	932.78	898.98	-	-	-	-	-	-
23.62	828.85	802.53	-	-	-	-	796.02	-
24.68	736.99	716.87	-	-	-	-	-	-
25.8	654.47	639.57	-	-	-	-	-	-
28.03	524.29	516.8	-	-	-	-	560.42	-
31.64	379.17	378.48	-	-	-	-	337.08	-
34.17	308.65	310.57	-	-	-	-	318.44	-
36.82	252.75	256.3	-	-	-	-	-	-
38.18	229.38	233.48	-	-	-	-	235.29	-
41	189.55	194.39	-	-	-	-	178.26	-
43.95	157.37	162.59	-	-	-	-	-	-
45.47	143.66	148.98	-	-	-	-	140.5	-
46.9	132.22	137.58	-	-	-	-	-	-
48.6	120.17	125.55	-	-	-	-	-	-
50.2	110.16	115.51	-	-	-	-	-	-
53.54	92.65	97.88	-	-	-	-	-	79.33
59.5	69.69	74.62	-	-	378.21	-	-	-
60.62	59.73	61.58	-	-	-	-	-	63.88
70.27	42.12	42.88	-	-	-	-	-	38.07
78.71	31.93	32.47	-	-	-	-	-	27.08
$_{51}$Sb								
31.64	1054.37	985.02	-	-	-	-	970.56	-
34.17	858.29	808.26	-	-	-	-	680.81	-
38.18	637.83	607.64	-	-	-	-	504.29	-
41	527.09	505.92	-	-	-	-	450.1	-
45.47	399.49	387.73	-	-	-	-	345.76	-
46.9	367.67	358.06	-	-	-	-	-	-
53.54	257.62	254.75	-	-	-	-	-	221.01
59.5	193.78	194.2	-	-	180.21	-	-	-
60.62	151.03	153.23	-	-	-	-	-	149.83
70.27	106.49	106.7	-	-	-	-	-	109.8
78.01	82.53	82.59	-	-	-	-		82.7

Table 4. Comparison of semi-empirical K_{tot} X-ray fluorescence cross-section (in barn) deduced from this work by photon impact with the experimental values literature and with empirical values of Amari *et al.* (2024b).

E(KeV)	Our results		Other Experimentales works				
		Empirical values	Experimentales Values				
	Semi-empirical values	Amari *et al.* (2024b)	Baydaş *et al.* (2003)	Rao *et al*. (1993)	Demir and Şahin (2013)	Singh *et al.* (1990)	Seven (2012)	Seven and Erdoğan (2015)
$_{28}$Ni								
8.74	9867.37	10149.26	9162	-	-	-	-	-
9.36	8279.75	8480.07	8479	-	-	-	-	-
10	6991.03	7130.03	6939	-	-	-	-	-
10.68	5908.84	6000.46	6501	-	-	-	-	-
11.4	5001.71	5057.09	5126	-	-	-	-	-
12.09	4304.87	4335	4386	-	-	-	-	-
13.6	3188.49	3184.08	3207	-	-	-	-	-
14.38	2766.07	2750.97	2778	-	-	-	-	-
15.2	2401.72	2378.71	2447	-	-	-	-	-
16.04	2094.39	2065.83	2349	-	-	-	-	-
17.8	1607.14	1572.35	-	-	-	-	-	-
22.6	876.33	840.82	-	-	-	-	-	-
23.62	783.42	748.93	-	616	-	-	-	-
24.68	700.8	667.51	-	567	-	-	-	-
25.8	626.11	594.19	-	-	-	-	-	-
32.86	338.36	315.15	-	-	-	-	-	-
36.82	252.88	233.86	-	199	-	-	-	-
41	191.66	176.41	-	-	-	-	-	-
43.95	159.98	147.03	-	134	-	-	-	-
46.9	134.91	124	-	-	-	-	-	-
59.5	70.76	66.45	-	-	53.86			
$_{38}$Sr								
17.8	7199.19	7395.55	-	-	-	7152	-	-
22.6	3925.53	3954.8	-	-	-	4296	-	-
23.62	3509.35	3522.59	-	-	-	-	3313.76	-
24.68	3139.24	3139.62	-	-	-	-	-	-
25.8	2804.67	2794.76	-	-	-	2794	-	-
28.03	2272.02	2248.8	-	-	-	-	2160.97	-
31.64	1669.22	1636.86	-	-	-	-	1541.86	-
34.17	1371.64	1337.9	-	-	-	-	1204.6	-
36.82	1132.78	1099.96	-	-	-	-	-	-
38.18	1031.94	1000.18	-	-	-	-	892.93	-
41	858.54	829.74	-	-	-	769	807.67	-
43.95	716.63	691.56	-	-	-	-	-	-
45.47	655.6	632.58	-	-	-	-	600.92	-
46.9	604.32	583.25	-	-	-	469	-	-
48.6	549.99	531.27	-	-	-	-	-	-

50.2	504.53	488.02	-	-	-	-	-	-
59.5	316.97	312.55	-	-	275.46	-	-	-
$_{42}$Mo								
21.57	6832.9	7013.97	-	-	-	-	6765.79	-
22.6	6069.76	6206.57	-	-	-	-	-	-
23.62	5426.26	5528.26	-	-	-	-	5302.62	-
24.68	4853.97	4927.25	-	-	-	-	-	-
25.8	4336.65	4386.02	-	-	-	-	-	-
28.03	3513.05	3529.22	-	-	-	-	3423.04	-
31.64	2580.99	2568.85	-	-	-	-	2645.34	-
34.17	2120.86	2099.66	-	-	-	-	2163.14	-
36.82	1751.53	1726.25	-	-	-	-	-	-
38.18	1595.61	1569.66	-	-	-	-	1555.41	-
41	1327.49	1302.17	-	-	-	-	1267.23	-
43.95	1108.07	1085.31	-	-	-	-	-	-
45.47	1013.71	992.75	-	-	-	-	937	-
46.9	934.41	915.35	-	-	-	-	-	-
48.6	850.41	833.76	-	-	-	-	-	-
50.2	780.12	765.88	-	-	-	-	-	-
53.54	655.89	646.87	-	-	-	-	-	581.13
59.5	490.11	490.5	-	-	454.88	-	-	-
60.62	406.25	405.25	-	-	-	-	-	383.28
70.27	281.82	277.89	-	-	-	-	-	261.09
78.71	210.67	208	-	-	-	-	-	202.31
$_{51}$Sb								
31.64	5450.25	5562.61	-	-	-	-	5892.11	-
34.17	4478.6	4546.63	-	-	-	-	4326.47	-
38.18	3369.43	3398.95	-	-	-	-	2975.17	-
41	2803.25	2819.72	-	-	-	-	2595.44	-
45.47	2140.64	2149.72	-	-	-	-	2053.34	-
46.9	1973.19	1982.09	-	-	-	-	-	-
53.54	1385.04	1400.74	-	-	-	-	-	1308.64
59.5	1034.96	1062.14	-	-	1030.35	-	-	-
60.62	887.03	890.51	-	-	-	-	-	914.15
70.27	615.35	610.65	-	-	-	-	-	589.01
78.01	470.79	467.62	-	-	-	-	-	466.07